Second-order Lagrangian interactions of tri-dimensional gravity waves.

Frédéric Nouguier[1]†, Bertrand Chapron[2] and Charles-Antoine Guérin[1]
[1]Université de Toulon, CNRS/INSU, IRD, Mediterranean Institute of Oceanography (MIO), UM 110, 83957 La Garde, France
[2]Laboratoire d'Océanographie Spatiale, Ifremer, 29280 Plouzané, France

(Received ?; revised ?; accepted ?. - To be entered by editorial office)

We revisit and extend the description of gravity waves based on a perturbation expansion in Lagrangian coordinates. A general analytical framework is developed to derive the second-order Lagrangian solution for the motion of arbitrary gravity surface wave fields in a compact and vector form. The result is shown to be consistent with the classical second-order Eulerian expansion by Longuet-Higgins (1963) and is used to improve the original derivation by Pierson (1961) for long-crested waves. As demonstrated, the Lagrangian perturbation expansion captures higher degrees of nonlinearities than the corresponding Eulerian expansion at same order. At second-order, it can account for complex nonlinear phenomena such as the initial stage of the horse-shoe patterns formation and Benjamin-Feir modulational instability to shed new light on the origin of these mechanisms.

Key words: Will be entered by the editorial office.

1. Introduction

The Lagrangian description of interactions between multiple gravity surface waves was pioneered by Pierson (1961) half a century ago. Pierson derived explicitly the first-order solution for two-dimensional surfaces and pushed the calculation to the second-order for long-crested surfaces. He showed that first-order results include more realistic features than the Eulerian counterpart, such as sharp crests and flat troughs. In this present work, we revisit and correct this historical study to provide a general analytical framework, and to derive a compact and vector form for the second-order Lagrangian description of arbitrary tri-dimensional gravity wave fields. The analysis of tri-dimensional multiple wave systems is much richer than long-crested surfaces and monochromatic waves as some geometrical and dynamical characteristics of the wave field can only be accounted for by considering interactions between different, non-aligned free wave vectors.

To date, exploration of the numerical and analytical possibilities opened by the Lagrangian formalism have been somehow overlooked. A renewed interest in Lagrangian approaches and their mathematical (Yakubovich & Zenkovich (2004); Buldakov *et al.* (2006); Clamond (2007)) or practical implications (Gjosund (2003); Fouques *et al.* (2006); Fouques & Stansberg (2009)) have been further highlighted to provide means to better evaluate the statistical and geometrical description of free surface and mass transport (Lindgren (2006); Aberg (2007); Aberg & Lindgren (2008); Nouguier *et al.* (2009); Socquet-Juglard *et al.* (2005); Hsu *et al.* (2010, 2012)). The underlying reason behind

† Email address for correspondence: frederic.nouguier@univ-tln.fr

these remarkable properties is that the Lagrangian representation is clearly adapted for describing steep waves and a very useful mathematical tool to correctly evaluate statistical quantities (such as height, slope and curvature distribution) of random gravity waves fields at a limited analytical complexity cost.

Our main finding is given by equation (4.45) which summarizes the Lagrangian expressions of the second order displacements of water particles and pressure in the whole fluid domain. The analysis is restricted to infinite depth but there is no conceptual difficulty in relaxing this assumption. Full consistency is shown with the second-order Eulerian expansion of Longuet-Higgins (1963). Pierson's (1961) original second-order Lagrangian solution for long-crested waves is discussed and adjusted to agree with Longuet-Higgins (1963) and our derivations. We further discuss two remarkable phenomena which are not captured by the second-order Eulerian expansions. Firstly, the formation of horse-shoe patterns was identified as the result of a non-isotropic drift current. Secondly, Benjamin-Feir modulational instability is also revealed to be already present in the second-order Lagrangian framework as a simple beat effect between two neighbor harmonics instead of an energy exchange between carrier and sideband waves.

2. Eulerian versus Lagrangian expansions

We consider an incompressible fluid of constant density ρ in infinite depth, subject to the sole restoring force of gravity (surface tension and viscosity are ignored). The pressure is set to be a constant p_a at the free surface of the fluid. We chose a fixed system of axis $(\widehat{\boldsymbol{x}},\ \widehat{\boldsymbol{y}},\ \widehat{\boldsymbol{z}})$ with upwards directed vertical vector $\widehat{\boldsymbol{z}}$.

2.1. *Eulerian description*

In the Eulerian description, any position in space is identified by its coordinate $(x,\ y,\ z)$, which can be decomposed into its horizontal projection $\boldsymbol{r} = (x,\ y)$ and vertical elevation z. The evolving field of gravity waves is described by its elevations $\eta(\boldsymbol{r}, t)$ and velocity potential $\underline{\Phi}(x,\ y,\ z,\ t)$ with t being the time variable. In the Eulerian coordinates the potential solves Laplace equation in the volume together with dynamic and kinematic conditions at the borders:

$$
\begin{aligned}
\Delta\underline{\Phi} &= 0,\ z < \eta(x,y,t) \\
\lim_{z\to-\infty} \nabla\underline{\Phi} &= 0, \\
\underline{\Phi}_t + \tfrac{1}{2}\nabla\underline{\Phi}\cdot\nabla\underline{\Phi} &= -g\eta,\ z = \eta(x,y,t) \\
\underline{\Phi}_z &= \eta_t + \nabla\eta\cdot\nabla\underline{\Phi},\ z = \eta(x,y,t),
\end{aligned}
\tag{2.1}
$$

where g is the acceleration due to gravity. In the classical perturbation approach (Hasselmann (1962); Longuet-Higgins (1963); Weber & Barrick (1977)) the field of elevation η and the velocity potential $\underline{\Phi}$ at position and time $(\boldsymbol{r}, t)$ are sought in the form:

$$
\begin{aligned}
\eta &= \eta_0 + \eta_1 + \eta_2 + ... \\
\underline{\Phi} &= \underline{\Phi}_0 + \underline{\Phi}_1 + \underline{\Phi}_2 + ...
\end{aligned}
\tag{2.2}
$$

The naught terms, η_0 and $\underline{\Phi}_0$, are the reference solutions corresponding to a flat fluid interface and the following terms, η_1 and $\underline{\Phi}_1$, are the solutions provided by the linearized equations. The successive terms, η_n and $\underline{\Phi}_n$, are corrections of order n with respect to a small parameter. In the general case of multiple waves, this small parameter is not well identified but can linked to the wave steepness in the case of a monochromatic wave.

2.2. *Lagrangian description*

In the Lagrangian approach (Lamb 1932), the fluid evolution is described by the motion of fluid particles. The spatial coordinates $\boldsymbol{R} = (x,\ y,\ z)$ of the particles now depend on their independent reference labels $\boldsymbol{\zeta} = (\alpha,\ \beta,\ \delta)$ and time t, that is explicitly $x = x(\alpha,\beta,\delta,t),\ y = y(\alpha,\beta,\delta,t)$ and $z = z(\alpha,\beta,\delta,t)$. We choose hereafter $\boldsymbol{\zeta}$ as the locus of particles at rest. For ease of reading we introduce dedicated notations for the horizontal component of particles labels and positions, $\boldsymbol{\xi} = (\alpha,\beta)$ and $\boldsymbol{r} = (x,\ y)$ respectively.

The evolution of particle coordinates is driven by Newton's law of dynamics:

$$\boldsymbol{R}_{tt} + g\widehat{\boldsymbol{z}} = -\frac{1}{\rho}\boldsymbol{\nabla}_{\boldsymbol{R}}p \tag{2.3}$$

where $p = p(\boldsymbol{R})$ is the local pressure. This dynamical equation is coupled with the continuity equation:

$$|\mathbb{J}| = 1; \qquad \frac{\partial}{\partial t}|\mathbb{J}| = 0 \quad \text{with} \quad \mathbb{J} = \begin{bmatrix} x_\alpha & y_\alpha & z_\alpha \\ x_\beta & y_\beta & z_\beta \\ x_\delta & y_\delta & z_\delta \end{bmatrix}. \tag{2.4}$$

Multiplying equation (2.3) by $\mathbb{J}$ leads to

$$\mathbb{J}\boldsymbol{R}_{tt} + g\boldsymbol{\nabla}(\boldsymbol{R}\cdot\widehat{\boldsymbol{z}}) + \frac{1}{\rho}\boldsymbol{\nabla}p = 0 \tag{2.5}$$

which is the basic equation given by Lamb (1932). From here on the spatial gradient relative to the independent Lagrangian variables (α,β,δ) will be noted $\boldsymbol{\nabla}$.

Solutions of these equations need not be irrotational. However, if a function $F(\boldsymbol{\zeta},\ t)$ can be found such that

$$dF = (\mathbb{J}\boldsymbol{R}_t)\cdot d\boldsymbol{\zeta} \tag{2.6}$$

is a perfect differential then there is no vorticity (see appendix A.1). Here $d\boldsymbol{\zeta} = (d\alpha, d\beta, d\delta)$ denotes an infinitesimal label variation. Following the methodology described by Stoker (1957) we may seek for the solution in the form of a simultaneous perturbation expansion for position, pressure and the vorticity function:

$$\begin{aligned} \boldsymbol{R} &= \boldsymbol{R}_0 + \boldsymbol{R}_1 + \boldsymbol{R}_2 + ... \\ p &= p_a - \rho g\delta + p_1 + p_2 + ... \\ F &= F_0 + F_1 + F_2 + ... \end{aligned} \tag{2.7}$$

where the naught variables refer to particles at rest.

3. First-order solution: the Gerstner wave

Let us map the fluid domain onto the strip $\delta \leqslant 0$. From now on, $\delta = 0$ corresponds to the free surface η with pressure p_a. The zeroth order solution in the expansion (2.7) is related to particles at rest and writes :

$$\begin{aligned} &\boldsymbol{R}_0 = \boldsymbol{\zeta}, \\ &p_0 = p_a - \rho g\delta \\ &F_0 = 0 \\ &|\mathbb{J}| = 1 \end{aligned} \tag{3.1}$$

First-order quantities are the solution of linearized Lagrangian equations. When taken at first-order, equation (2.5) writes:

$$\boldsymbol{R}_{1tt} + g\boldsymbol{\nabla}(\boldsymbol{R}_1 \cdot \widehat{\boldsymbol{z}}) + \frac{1}{\rho}\boldsymbol{\nabla} p_1 = 0. \tag{3.2}$$

and the continuity equation is expressed by:

$$x_{1\alpha} + y_{1\beta} + z_{1\delta} = \boldsymbol{\nabla} \cdot \boldsymbol{R}_1 = 0. \tag{3.3}$$

In order to simplify the calculations presented in the next section and to ensure an irrotational solution at first order (see equation (3.9) below), we investigate solutions of the form $\boldsymbol{R}_1 = \boldsymbol{\nabla} w$ where $w(\boldsymbol{\zeta}, t)$ is a function to be found. This last quantity must satisfy the following equation:

$$\boldsymbol{\nabla}\left(w_{tt} + g w_\delta + p_1/\rho\right) = 0. \tag{3.4}$$

With $p_1 = 0$ at $\delta = 0$ this leads to the solution:

$$w = \cos(\boldsymbol{k} \cdot \boldsymbol{\xi} - \omega t)e^{k\delta}; \qquad \omega^2 = gk; \qquad p_1 = 0. \tag{3.5}$$

where $\boldsymbol{k} = (k_\alpha,\ k_\beta)$ is an independent bi-dimensional vector in the $(\alpha,\ \beta)$ domain and k a constant parameter. At first order in ϵ, the relation of continuity (3.3) writes

$$\Delta w = (-k_\alpha^2 - k_\beta^2 + k^2)w = 0 \tag{3.6}$$

leading to $||\boldsymbol{k}|| = k$. As $\boldsymbol{R}_1$ is a spatial displacement, a suitable solution is $\boldsymbol{R}_1 = \boldsymbol{\nabla}(ak^{-1}w)$ which leads to the first-order solution :

$$\left\{\begin{array}{lcl} \boldsymbol{r} & = & \boldsymbol{\xi} - a\widehat{\boldsymbol{k}}\sin(\boldsymbol{k} \cdot \boldsymbol{\xi} - \omega t)e^{k\delta} \\ z & = & \delta + a\cos(\boldsymbol{k} \cdot \boldsymbol{\xi} - \omega t)e^{k\delta} \\ p & = & p_0 - \rho g \delta \end{array}\right. . \tag{3.7}$$

From here on, we use the notation $\widehat{\boldsymbol{k}} = \boldsymbol{k}/k$ for the direction of a vector $\boldsymbol{k}$ and k for its norm. This solution describes water particles trajectories as circles with radius decreasing exponentially with water depth. The spatial profile of such waves is a trochoid moving in the direction $\boldsymbol{k}$ with a crest to trough wave amplitude defined by the circle radius a of particles trajectories at the free surface.

Two centuries ago, Gerstner (1809) derived an exact solution of the equation of motion (2.3) and obtained the same solution (3.7) for water particle trajectories $(\boldsymbol{r}, z)$ with, however, a slightly different pressure term:

$$p = p_0 - \rho g \delta + \tfrac{1}{2}k^{-2}\rho\omega^2 e^{2k\delta}. \tag{3.8}$$

The Gerstner wave has been described in classical textbooks (e.g. Lamb (1932); Kinsman (1965)) even though its stability was investigated only recently (Naciri & Mei (1992); Leblanc (2004)). It has always been criticized in view of its non-vanishing vorticity. This calls for some discussion on the presence of vorticity. Wind waves do in general have vorticity, although it is indeed small. The main reason for which most of the studies have been devoted to irrotational waves is the considerable simplification offered by potential theory in the analytical derivations. It turns out that the predictions of potential theory agree reasonably well with the observations, which does not mean that real waves are irrotational but rather that vorticity has only secondary effects. However, discrepancies are bound to become visible as the quality and accuracy of observations improve and it will soon become necessary to account for vorticity. The main shortcoming of Gerstner solution is that it does not address a wide class of solutions with small vorticity. Its vorticity has indeed a very special distribution and there is no rationale why it should be more relevant than any other of the same order. In the present analytical framework, the construction of a weakly nonlinear solution to the exact inviscid equations is more general and it is possible to examine arbitrary distributions with small vorticity and evaluate, at least coarsely, the importance if this effect.

As already derived by Pierson (1961), equation (2.6) writes at first order in ϵ:

$$dF = \boldsymbol{R}_{1t} \cdot d\boldsymbol{\zeta} \tag{3.9}$$

which is a perfect differential of F_1 since $dF = \boldsymbol{\nabla} F_1 \cdot d\boldsymbol{\zeta}$ with

$$F_1 = ak^{-1}w_t = \frac{a\omega}{k}\sin(\boldsymbol{k}\cdot\boldsymbol{\xi} - \omega t)e^{k\delta}. \tag{3.10}$$

Therefore, there is no vorticity at first order and the Gerstner wave (with the corresponding pressure given by equation (3.7)) is an irrotational solution at the considered order of the expansion.

Because of the linearity of equation (2.5), we can write an extended solution of the first-order equations as a continuous superposition of independent harmonics defined by their wavenumber $\boldsymbol{k}$ in the form:

$$\boldsymbol{R}_1 = \boldsymbol{\nabla}\Phi_1 \quad \text{with} \quad \Phi_1 = \phi_1 + c.c., \tag{3.11}$$

where "c.c." designates the complex conjugate of a given quantity and

$$\phi_1 = \frac{1}{2}\int_{\Re^2} \frac{A(\boldsymbol{k})}{k} e^{i(\boldsymbol{k}\cdot\boldsymbol{\xi} - \omega t)} e^{k\delta} d\boldsymbol{k}. \tag{3.12}$$

Here $A(\boldsymbol{k})$ is the orbital amplitude and the factor $\frac{1}{2}$ accounts for the complex plus conjugate formulation of Φ_1. Such an orbital spectrum has been already introduced in the statistical studies of Lagrangian wave fields (Pierson (1961); Lindgren & Lindgren (2011); Daemrich & Woltering (2008)) and describes the spectral content of the particle motion. It is sometimes termed "undressed" spectrum (Elfouhaily *et al.* (1999)) when it refers to a nonlinear transformation of an underlying linear surface (Creamer *et al.* (1989)).

In the present state of knowledge, establishing the relationship between the orbital (Lagrangian) and the surface (Eulerian) spectrum is still an issue. When the amplitude $A(\boldsymbol{k})$ is taken to be a complex random variables with independent uniformly distributed random phases, the resulting function ϕ_1 is a complex random Gaussian process by virtue of the law of large numbers. However, the random surface η defined by the locus of particles at the free surface is no longer Gaussian. This implies that the corresponding distribution of elevation, slopes and curvatures distributions deviate from the Normal distribution. Statistical properties of such random wave fields have been studied in detail (e.g. Pierson (1961); Gjosund (2003); Aberg & Lindgren (2008); Nouguier *et al.* (2009); Lindgren & Aberg (2009); Lindgren & Lindgren (2011)) and were found to be more consistent with ocean wave field measurements. *A contrario*, it should ne noted that a first-order expansion in the Eulerian framework, which expresses the surface and its derivatives as a linear superposition of free harmonics, is bound to the Gaussian statistics.

4. Second-order Lagrangian solution

This section is devoted to the second-order Lagrangian expansion. We recall the corresponding equations and detail the calculations to derive the second-order displacements and the pressure terms as function of the Lagrangian variables. To simplify the notations we omit the integration elements ($d\boldsymbol{k}$, $d\boldsymbol{k'}$) and domain ($\Re^2$ and $\Re^2 \times \Re^2$) in the following single and double integrals.

4.1. *Second-order equations*

Retaining the second-order terms in (2.5) we obtain:

$$\boldsymbol{R}_{2tt} + g\boldsymbol{\nabla} z_2 + \boldsymbol{\nabla} p_2/\rho = -\mathcal{H}(\Phi_1)\boldsymbol{\nabla}\Phi_{1tt}, \tag{4.1}$$

where $\mathcal{H}$ is the Hessian operator, that is the square matrix built with the second-order partial derivatives relative to the (α, β, δ) variables:

$$\mathcal{H}(\Phi_1) = \begin{bmatrix} \partial^2_{\alpha\alpha} & \partial^2_{\alpha\beta} & \partial^2_{\alpha\delta} \\ \partial^2_{\beta\alpha} & \partial^2_{\beta\beta} & \partial^2_{\beta\delta} \\ \partial^2_{\delta\alpha} & \partial^2_{\delta\beta} & \partial^2_{\delta\delta} \end{bmatrix} \Phi_1 \tag{4.2}$$

For practical purposes we rewrite the right-hand side of (4.1) as:

$$-\mathcal{H}(\Phi_1)\boldsymbol{\nabla}\Phi_{1tt} = \boldsymbol{S} + \boldsymbol{T} \tag{4.3}$$

with

$$\boldsymbol{S} = (S^\alpha, S^\beta, S^\delta) = -\mathcal{H}(\phi_1)\boldsymbol{\nabla}\phi_{1tt} + c.c. \tag{4.4}$$

$$\boldsymbol{T} = (T^\alpha, T^\beta, T^\delta) = -\mathcal{H}(\phi_1)\boldsymbol{\nabla}\phi^*_{1tt} + c.c. \tag{4.5}$$

where the superscript '$*$' refers to the complex conjugate. Straightforward derivations given in the appendix A.2 leads to:

$$\left\{ \begin{array}{lcl} (S^\alpha, S^\beta) & = & \iint \mathcal{N}\, gkk' \frac{i}{2}(\widehat{\boldsymbol{k}} + \widehat{\boldsymbol{k'}}) + c.c. \\ S^\delta & = & \iint \mathcal{N}\, gkk' + c.c. \end{array} \right. \quad \text{and} \quad \left\{ \begin{array}{lcl} (T^\alpha, T^\beta) & = & \iint \underline{\mathcal{N}}\, gkk' \frac{i}{2}(\widehat{\boldsymbol{k}} - \widehat{\boldsymbol{k'}}) + c.c. \\ T^\delta & = & \iint \underline{\mathcal{N}}\, gkk' + c.c. \end{array} \right. \tag{4.6}$$

where the kernels $\mathcal{N}$ and $\underline{\mathcal{N}}$ depend on the variables $\boldsymbol{k}$, $\boldsymbol{k}'$, $\boldsymbol{\xi}$, δ and t and are defined as follows:

$$\mathcal{N} = \mathcal{B}e^{-i(\omega+\omega')t}\ e^{(k+k')\delta} \quad \text{and} \quad \underline{\mathcal{N}} = \underline{\mathcal{B}}e^{-i(\omega-\omega')t}\ e^{(k+k')\delta}. \tag{4.7}$$

with

$$\mathcal{B}(\boldsymbol{k}, \boldsymbol{k}', \boldsymbol{\xi}) = \tfrac{1}{4}(1 - \widehat{\boldsymbol{k}} \cdot \widehat{\boldsymbol{k}}')A(\boldsymbol{k})A(\boldsymbol{k}')e^{i(\boldsymbol{k}+\boldsymbol{k}')\cdot\boldsymbol{\xi}} \tag{4.8}$$

$$\underline{\mathcal{B}}(\boldsymbol{k}, \boldsymbol{k}', \boldsymbol{\xi}) = \tfrac{1}{4}(1 + \widehat{\boldsymbol{k}} \cdot \widehat{\boldsymbol{k}}')A(\boldsymbol{k})A^*(\boldsymbol{k}')e^{i(\boldsymbol{k}-\boldsymbol{k}')\cdot\boldsymbol{\xi}}. \tag{4.9}$$

Analogously, the continuity equation (2.4) at second-order writes:

$$x_{2\alpha} + y_{2\beta} + z_{2\delta} + \Phi_{1\alpha\alpha}\Phi_{1\beta\beta} + \Phi_{1\alpha\alpha}\Phi_{1\delta\delta} + \Phi_{1\beta\beta}\Phi_{1\delta\delta} - \Phi^2_{1\alpha\beta} - \Phi^2_{1\alpha\delta} - \Phi^2_{1\beta\delta} = 0 \tag{4.10}$$

and can be rewritten in the form (see appendix A.3):

$$\boldsymbol{\nabla} \cdot \boldsymbol{R}_2 = V + W \tag{4.11}$$

with

$$V = \iint \tfrac{1}{2}(kk' - \boldsymbol{k}\cdot\boldsymbol{k}')\mathcal{N} + c.c. \qquad \text{and} \qquad W = \iint \tfrac{1}{2}(kk' + \boldsymbol{k}\cdot\boldsymbol{k}')\underline{\mathcal{N}} + c.c. \tag{4.12}$$

4.2. *Second-order expressions*

Due to the linearity of (4.1) and (4.11), we first consider the solution of equation (4.1) with the sole $\boldsymbol{S}$ term on the right-hand side, that is:

$$\boldsymbol{R}_{2tt} + g\boldsymbol{\nabla} z_2 + \boldsymbol{\nabla} p_2/\rho = \boldsymbol{S}. \tag{4.13}$$

We furthermore assume that $\boldsymbol{r}_2, z_2$ and p_2 can be written as the following integrals:

$$\boldsymbol{r}_2 = \iint \mathcal{N}\ i\boldsymbol{\mathcal{R}} + c.c. \tag{4.14}$$

$$z_2 = \iint \mathcal{N}\ \mathcal{Z} + c.c. \tag{4.15}$$

$$p_2 = \rho g \iint \mathcal{N}\ \mathcal{P} + c.c., \tag{4.16}$$

where $\boldsymbol{\mathcal{R}}$, $\mathcal{Z}$ and $\mathcal{P}$ are unknown kernels depending on $\boldsymbol{k}$ and $\boldsymbol{k}'$. Inserting these expressions in (4.13) leads to a set of equations for the kernels:

$$\left\{ \begin{array}{rcl} -\mathcal{Z}\Omega^+ + (\mathcal{Z}+\mathcal{P})(k+k') &=& kk' \\ -\Omega^+\boldsymbol{\mathcal{R}} + (\boldsymbol{k}+\boldsymbol{k}')(\mathcal{Z}+\mathcal{P}) &=& \frac{1}{2}kk'(\widehat{\boldsymbol{k}}+\widehat{\boldsymbol{k}'}), \end{array} \right. \tag{4.17}$$

where we have defined:

$$\Omega^{\pm} = \left(\sqrt{k} \pm \sqrt{k'}\right)^2. \tag{4.18}$$

Inserting again equations (4.14)-(4.16) in (4.11) and keeping only the terms involving the kernel $\mathcal{N}$ leads to a third equation:

$$-\boldsymbol{\mathcal{R}}\cdot(\boldsymbol{k}+\boldsymbol{k}') + \mathcal{Z}(k+k') = \tfrac{1}{2}(kk' - \boldsymbol{k}\cdot\boldsymbol{k}') \tag{4.19}$$

Equations (4.17) and (4.19) can easily be solved leading to:

$$\left\{ \begin{array}{rcl} \boldsymbol{\mathcal{R}} &=& \dfrac{\omega\boldsymbol{k}+\omega'\boldsymbol{k}'}{2(\omega+\omega')} \\ \mathcal{Z} &=& \frac{1}{4}\left(k+k'+\Omega^-\right) \\ \mathcal{P} &=& \sqrt{kk'} \end{array} \right. \tag{4.20}$$

Analogously, we solve equation (4.1) with the sole $\boldsymbol{T}$ term on the right-hand side, that is:

$$\boldsymbol{R}_{2tt} + g\boldsymbol{\nabla} z_2 + \boldsymbol{\nabla} p_2/\rho = \boldsymbol{T}. \tag{4.21}$$

Again, we assume that $\boldsymbol{r}_2, z_2$ and p_2 can be found in the form given in equations (4.14), (4.15) and (4.16) with some other kernels $\underline{\mathcal{N}}$, $\underline{\boldsymbol{\mathcal{R}}}$, $\underline{\mathcal{Z}}$ and $\underline{\mathcal{P}}$. Since equation (4.11) involving the kernel $\mathcal{N}$ was already solved, the only remaining terms are those involving $\underline{\mathcal{N}}$ in equation (4.11). A set of three equations is thus obtained for the unknown kernels:

$$\left\{ \begin{array}{rcl} -\underline{\mathcal{Z}}\Omega^- + (\underline{\mathcal{Z}}+\underline{\mathcal{P}})(k+k') &=& kk' \\ -\Omega^-\underline{\boldsymbol{\mathcal{R}}} + (\boldsymbol{k}-\boldsymbol{k}')(\underline{\mathcal{Z}}+\underline{\mathcal{P}}) &=& \frac{1}{2}kk'(\widehat{\boldsymbol{k}}-\widehat{\boldsymbol{k}'} \\ -\underline{\boldsymbol{\mathcal{R}}}\cdot(\boldsymbol{k}-\boldsymbol{k}') + \underline{\mathcal{Z}}(k+k') &=& \frac{1}{2}(kk'+\boldsymbol{k}\cdot\boldsymbol{k}') \end{array} \right. \tag{4.22}$$

Again, this system can easily be solved leading to:

$$\left\{ \begin{array}{l} \underline{\boldsymbol{\mathcal{R}}} = \dfrac{\omega\boldsymbol{k}+\omega'\boldsymbol{k}'}{2(\omega-\omega')} \\ \underline{\mathcal{Z}} = \frac{1}{4}\left(k+k'+\Omega^+\right) \\ \underline{\mathcal{P}} = -\sqrt{kk'} \end{array} \right. \quad \text{if } \omega \neq \omega'; \tag{4.23}$$

The case $\omega = \omega'$ will be discussed in detail in section 4.3. At this point we have found a solution of the second-order Lagrangian expansion (4.1) in the form:

$$\boldsymbol{r}_2 = \iint i\left(\mathcal{N}\boldsymbol{\mathcal{R}} + \underline{\mathcal{N}}\underline{\boldsymbol{\mathcal{R}}}\right) + c.c. \tag{4.24}$$

$$z_2 = \iint \left(\mathcal{N}\mathcal{Z} + \underline{\mathcal{N}}\underline{\mathcal{Z}}\right) + c.c. \tag{4.25}$$

$$p_2 = \rho g \iint \left(\mathcal{N}\mathcal{P} + \underline{\mathcal{N}}\underline{\mathcal{P}}\right) + c.c. \tag{4.26}$$

However, the expression of p_2 does not satisfy to the boundary condition $p_2 = 0$ at $\delta = 0$ and needs to be corrected. Noting that $\mathcal{N} = \mathcal{B}e^{-i(\omega+\omega')t}\ e^{(k+k')\delta}$ and $\underline{\mathcal{N}} = \underline{\mathcal{B}}e^{-i(\omega-\omega')t}\ e^{(k+k')\delta}$, a very simple way to satisfy to the boundary condition is to complete p_2 in the form:

$$p_2 = \rho g \iint \mathcal{P}\mathcal{B}e^{-i(\omega+\omega')t}\left(e^{(k+k')\delta} - e^{K^+\delta}\right) + \underline{\mathcal{P}}\underline{\mathcal{B}}e^{-i(\omega-\omega')t}\left(e^{(k+k')\delta} - e^{K^-\delta}\right) + c.c.$$

where the additional kernels K^+ and K^- must be determined. The pressure at second-order can thus be written as:

$$p_2 = \iint \left((\mathcal{N} - \mathcal{N}')\mathcal{P} + (\underline{\mathcal{N}} - \underline{\mathcal{N}'})\underline{\mathcal{P}}\right) + c.c. \tag{4.27}$$

where we have introduced the two kernels $\mathcal{N}'$ and $\underline{\mathcal{N}'}$, which only differ from $\mathcal{N}$ and $\underline{\mathcal{N}}$, respectively, by the real exponential term:

$$\mathcal{N}' = \mathcal{B}e^{-i(\omega+\omega')t}\ e^{K^+\delta} \qquad \text{and} \qquad \underline{\mathcal{N}'} = \underline{\mathcal{B}}e^{-i(\omega-\omega')t}\ e^{K^-\delta}. \tag{4.28}$$

It is therefore natural to assume a complete expression of $\boldsymbol{r}_2$ and z_2 in the form:

$$\boldsymbol{r}_2 = \iint i\left(\mathcal{N}\boldsymbol{\mathcal{R}} - \mathcal{N}'\boldsymbol{\mathcal{R}'} + \underline{\mathcal{N}}\underline{\boldsymbol{\mathcal{R}}} - \underline{\mathcal{N}'}\underline{\boldsymbol{\mathcal{R}'}}\right) + c.c. \tag{4.29}$$

$$z_2 = \iint \left(\mathcal{N}\mathcal{Z} - \mathcal{N}'\mathcal{Z}' + \underline{\mathcal{N}}\underline{\mathcal{Z}} - \underline{\mathcal{N}'}\underline{\mathcal{Z}'}\right) + c.c., \tag{4.30}$$

where the primed kernels need to be found. To achieve this, we recall these expressions in (4.1) and identify the terms pertaining to the $\mathcal{N}'$ kernel only. This leads to the equations:

$$-\Omega^+\mathcal{Z}' + K^+(\mathcal{Z}' + P) = 0 \tag{4.31}$$

$$-\Omega^+\boldsymbol{\mathcal{R}'} + (\boldsymbol{k} + \boldsymbol{k}')(\mathcal{Z}' + P) = 0, \tag{4.32}$$

as well as:

$$-\boldsymbol{\mathcal{R}'}\cdot(\boldsymbol{k} + \boldsymbol{k}') + K^+\mathcal{Z}' = 0 \tag{4.33}$$

from the continuity equation. Inserting (4.31) in (4.32) and multiplying by $(\boldsymbol{k} + \boldsymbol{k}')/\Omega^+$ leads to

$$-\boldsymbol{\mathcal{R}'}\cdot(\boldsymbol{k} + \boldsymbol{k}') + \frac{||\boldsymbol{k} + \boldsymbol{k}'||^2}{K^+}\mathcal{Z}' = 0 \tag{4.34}$$

which is consistent with (4.33) if and only if:

$$K^+ = ||\boldsymbol{k} + \boldsymbol{k}'|| \tag{4.35}$$

(we discard the mathematical solution $K^+ = -||\boldsymbol{k} + \boldsymbol{k}'||$ which is nonphysical because of the asymptotic constraint $p_2 \to 0$ when $\delta \to -\infty$). We can now solve equations (4.31) and (4.32) to obtain:

$$\left\{\begin{array}{lcl} \boldsymbol{\mathcal{R}'} & = & \dfrac{\sqrt{kk'}(\boldsymbol{k}+\boldsymbol{k}')}{\Omega^{+}-||\boldsymbol{k}+\boldsymbol{k}'||} \\ \mathcal{Z}' & = & \dfrac{\sqrt{kk'}||\boldsymbol{k}+\boldsymbol{k}'||}{\Omega^{+}-||\boldsymbol{k}+\boldsymbol{k}'||} \end{array}\right. \tag{4.36}$$

Repeating the same procedure with the kernel $\underline{\mathcal{N}}'$ leads to another set of equations:

$$\left\{\begin{array}{rcl} -\Omega^{-}\underline{\mathcal{Z}'}+K^{-}(\underline{\mathcal{Z}'}+\underline{P}) & = & 0 \\ -\Omega^{-}\underline{\boldsymbol{\mathcal{R}'}}+(\boldsymbol{k}-\boldsymbol{k}')(\underline{\mathcal{Z}'}+\underline{P}) & = & 0 \\ -\underline{\boldsymbol{\mathcal{R}'}}\cdot(\boldsymbol{k}-\boldsymbol{k}')+K^{-}\underline{\mathcal{Z}'} & = & 0 \end{array}\right. \tag{4.37}$$

which admit the solution $K^{-}=||\boldsymbol{k}-\boldsymbol{k}'||$ and

$$\left\{\begin{array}{lcl} \underline{\boldsymbol{\mathcal{R}'}} & = & \dfrac{-\sqrt{kk'}(\boldsymbol{k}-\boldsymbol{k}')}{\Omega^{-}-||\boldsymbol{k}-\boldsymbol{k}'||} \\ \underline{\mathcal{Z}'} & = & \dfrac{-\sqrt{kk'}||\boldsymbol{k}-\boldsymbol{k}'||}{\Omega^{-}-||\boldsymbol{k}-\boldsymbol{k}'||} \end{array}\right. \tag{4.38}$$

4.3. *Interaction of harmonics with the same frequencies*

The complete kernels involved in the integral representation of $\boldsymbol{R}_2$ and p_2 have now been found. However, to complete the solution of the second-order Lagrangian equations we need to discuss the case $\omega=\omega'$ which has first been discarded in equation (4.23).

A generalized expression of the horizontal second-order term corresponding to kernel solutions (4.23) for the case $\omega=\omega'$ would be written as the limit:

$$\underline{\boldsymbol{r}}_2=\lim_{\gamma\to 0}\iint\limits_{\Re^4-\mathcal{E}} i\underline{\boldsymbol{\mathcal{R}}\mathcal{N}}+c.c. \tag{4.39}$$

where $\mathcal{E}$ is the $\Re^4$ subdomain such as $|\omega-\omega'|<\gamma$ and where $\underline{\boldsymbol{\mathcal{R}}}$, defined at equation (4.23), contains a singularity at $\omega=\omega'$. If this integral admits a finite value, it has to be defined in the sense of Cauchy Principal Value (PV):

$$\underline{\boldsymbol{r}}_2=PV\iint\limits_{\Re^4} i\frac{\omega\boldsymbol{k}+\omega'\boldsymbol{k}'}{2(\omega-\omega')}\underline{\mathcal{B}}e^{-i(\omega-\omega')t}e^{(k+k')\delta}+c.c. \tag{4.40}$$

The existence of the finite limit (4.39) is shown in appendix B ensuring that equation (4.40) is the correct expression of $\underline{\boldsymbol{r}}_2$.

4.4. *Second-order vorticity*

A complete Lagrangian second-order solution has now been found. We can verify *a posteriori* that it is indeed irrotational. For this, we have to investigate the second-order expression of the function dF, that is:

$$dF_2=[\boldsymbol{R}_{2t}+\mathcal{H}(\Phi_1)\boldsymbol{\nabla}(\Phi_{1t})]\cdot d\boldsymbol{\zeta}, \tag{4.41}$$

which we chose to rewrite in the form:

$$dF_2=\int_t dt\,[\boldsymbol{R}_{2tt}+\mathcal{H}(\Phi_1)\boldsymbol{\nabla}(\Phi_{1tt})+\mathcal{H}(\Phi_{1t})\boldsymbol{\nabla}(\Phi_{1t})]\cdot d\boldsymbol{\zeta} \tag{4.42}$$

where the symbol $\int_t dt$ refers to temporal integration. Inserting (4.1) in this last expression leads to:

$$dF_2=\boldsymbol{\nabla}\left[\int_t dt\left(-(gz_2+p_2/\rho)+\tfrac{1}{2}(\Phi_{1t})^2\right)\right]\cdot d\boldsymbol{\zeta}. \tag{4.43}$$

This provides F_2 in the form:

$$F_2 = \int_t dt \left(\tfrac{1}{2}(\Phi_{1t})^2 - gz_2 - p_2/\rho\right). \tag{4.44}$$

The existence of such a function F_2 warrants the absence of vorticity at the second order.

4.5. *Second-order solution*

To summarize all the expressions established previously, we can write the general solution of the second-order terms of equation (2.7) as follows:

$$\left\{\begin{array}{lll}
\boldsymbol{r}_2 & = & \displaystyle\iint i\left(\frac{\omega\boldsymbol{k}+\omega'\boldsymbol{k}'}{2(\omega+\omega')}e^{(k+k')\delta} - \frac{\sqrt{kk'}(\boldsymbol{k}+\boldsymbol{k}')}{\Omega^+ - ||\boldsymbol{k}+\boldsymbol{k}'||}e^{||\boldsymbol{k}+\boldsymbol{k}'||\delta}\right)\mathcal{B}e^{-i(\omega+\omega')t} + c.c. \\
 & +PV & \displaystyle\iint i\left(\frac{\omega\boldsymbol{k}+\omega'\boldsymbol{k}'}{2(\omega-\omega')}e^{(k+k')\delta} + \frac{\sqrt{kk'}(\boldsymbol{k}-\boldsymbol{k}')}{\Omega^- - ||\boldsymbol{k}-\boldsymbol{k}'||}e^{||\boldsymbol{k}-\boldsymbol{k}'||\delta}\right)\underline{\mathcal{B}}e^{-i(\omega-\omega')t} + c.c. \\
z_2 & = & \displaystyle\iint \left(\frac{k+k'+\Omega^-}{4}e^{(k+k')\delta} - \frac{\sqrt{kk'}||\boldsymbol{k}+\boldsymbol{k}'||}{\Omega^+ - ||\boldsymbol{k}+\boldsymbol{k}'||}e^{||\boldsymbol{k}+\boldsymbol{k}'||\delta}\right)\mathcal{B}e^{-i(\omega+\omega')t} + c.c. \\
 & + & \displaystyle\iint \left(\frac{k+k'+\Omega^+}{4}e^{(k+k')\delta} + \frac{\sqrt{kk'}||\boldsymbol{k}-\boldsymbol{k}'||}{\Omega^- - ||\boldsymbol{k}-\boldsymbol{k}'||}e^{||\boldsymbol{k}-\boldsymbol{k}'||\delta}\right)\underline{\mathcal{B}}e^{-i(\omega-\omega')t} + c.c. \\
p_2 & = & \displaystyle\rho g\iint \sqrt{kk'}\left(e^{(k+k')\delta} - e^{||\boldsymbol{k}+\boldsymbol{k}'||\delta}\right)\mathcal{B}e^{-i(\omega+\omega')t} + c.c. \\
 & - & \displaystyle\rho g\iint \sqrt{kk'}\left(e^{(k+k')\delta} - e^{||\boldsymbol{k}-\boldsymbol{k}'||\delta}\right)\underline{\mathcal{B}}e^{-i(\omega-\omega')t} + c.c.
\end{array}\right. \tag{4.45}$$

where $\mathcal{B}$ and $\underline{\mathcal{B}}$ are defined in equations (4.8) and (4.9) and $\Omega^\pm$ in equation (4.18).

5. Comparison with classical models

5.1. *Consistency with the Eulerian approach of M.S. Longuet-Higgins*

Before we investigate the consistency with classical Eulerian models, it is instructive to establish the correspondence between Eulerian and Lagrangian expansions. We consider the surface $\eta(\boldsymbol{r}, t)$ implicitly defined by the locus of particle trajectories $(\boldsymbol{r}(t),\ z(t))$ and we denote $\eta = \eta_0 + \eta_1 + \eta_2 + ...$ as its Eulerian expansion in order of steepness above some reference plane. Applying successive Taylor expansions and making use of the correspondence between the $(\alpha,\ \beta,\ \delta)$ Lagrangian labels and the $(x,\ y,\ z)$ coordinates system of the Eulerian description, it can be easily shown that:

$$\begin{aligned}
\eta_0 &= z_0 \\
\eta_1 &= z_1 - \boldsymbol{r}_1 \cdot \boldsymbol{\nabla}_{\boldsymbol{\xi}}\eta_0 \\
\eta_2 &= z_2 - \boldsymbol{r}_1 \cdot \boldsymbol{\nabla}_{\boldsymbol{\xi}}\eta_1 - \boldsymbol{r}_2 \cdot \boldsymbol{\nabla}_{\boldsymbol{\xi}}\eta_0 - \frac{1}{2}\boldsymbol{r}_1\boldsymbol{\nabla}_{\boldsymbol{\xi}}\boldsymbol{\nabla}_{\boldsymbol{\xi}}\eta_0\boldsymbol{r}_1 \\
\eta_n &= z_n - ...
\end{aligned} \tag{5.1}$$

where $\boldsymbol{\nabla}_{\boldsymbol{\xi}}$ is the horizontal bi-dimensional gradient and $\boldsymbol{\nabla}_{\boldsymbol{\xi}}\boldsymbol{\nabla}_{\boldsymbol{\xi}}$ the corresponding Hessian. The expansion can in principle be pursued at arbitrary order even though it becomes algebraically more complex. From this it is seen than any nth-order term in surface elevation (η_n) can be obtained from the combination of an nth-order term in vertical particle position (z_n) and lower-order terms $(\boldsymbol{r}_p, z_p)$, $p \leqslant n-1$. Hence, any given order of the Lagrangian expansion provides the complete corresponding Eulerian order and, is moreover involved in higher-order Eulerian terms.

The classical Eulerian approach (Hasselmann (1962); Longuet-Higgins (1963)) to the non-linear theory of gravity waves consist in seeking both the elevation η and the velocity potential $\underline{\Phi}$ at the free surface in a perturbation series (2.2). The expansion is usually performed about the mean horizontal plane of the leading order η_0 so that no zeroth-order term is present:

$$\eta(\boldsymbol{\xi},t) = \eta_1(\boldsymbol{\xi},t) + \eta_2(\boldsymbol{\xi},t) + ... \tag{5.2}$$
$$\underline{\Phi}(\boldsymbol{\xi},t) = \underline{\Phi}_1(\boldsymbol{\xi},t) + \underline{\Phi}_2(\boldsymbol{\xi},t) + ... \tag{5.3}$$

In these two equations and the rest of this section, the fixed Eulerian coordinates system (x,y) has been simply replaced by the (α,β) one. The first-order terms are given by the classical spectral representation,

$$\eta_1(\boldsymbol{\xi},t) = \sum_{j=1}^{N} a_j \cos\psi_j, \quad \psi_j = \boldsymbol{k_j}\cdot\boldsymbol{\xi} - \omega_j t + \varphi_j \tag{5.4}$$
$$\Phi_1(\boldsymbol{\xi},t) = \sum_{j=1}^{N} b_j \cos\psi_j, \tag{5.5}$$

where φ_j is the phase associated to the $\boldsymbol{k}_j$ component. The higher-order terms in the expansion involve nth order multiplicative combinations of these spectral components. The perturbation expansions of elevation and velocity potential are identified simultaneously by injecting the successive Fourier expansions in Navier-Stokes equations. The leading, quadratic, non-linear term for elevation was provided by Longuet-Higgins (1963) in the form†:

$$\eta_2(\boldsymbol{\xi},t) = \frac{1}{2}\sum_{i,j=1}^{N} a_i a_j \left[K_{ij}\cos\psi_i\cos\psi_j + K'_{ij}\sin\psi_i\sin\psi_j\right], \tag{5.6}$$

$$\begin{aligned} K_{ij} &= (k_i k_j)^{-\frac{1}{2}}\left[B^-_{ij} + B^+_{ij} - \boldsymbol{k_i}\cdot\boldsymbol{k_j}\right] + k_i + k_j \\ K'_{ij} &= (k_i k_j)^{-\frac{1}{2}}\left[B^-_{ij} - B^+_{ij} - k_i k_j\right] \\ B^{\pm}_{ij} &= \frac{\Omega^{\pm}_{ij}(\boldsymbol{k_i}\cdot\boldsymbol{k_j} \mp k_i k_j)}{\Omega^{\pm}_{ij} - ||\boldsymbol{k}_i \pm \boldsymbol{k}_j||} \\ \Omega^{\pm}_{ij} &= (\sqrt{k_i} \pm \sqrt{k_j})^2 \end{aligned} \tag{5.7}$$

and as usual $k = ||\boldsymbol{k}||$. The first-order Lagrangian expansion was shown to be close but not perfectly consistent with the second-order Eulerian perturbation expansion of Longuet-Higgins (see Nouguier *et al.* (2009)). We will now show that full consistency is achieved with the second-order Lagrangian expansion at the surface, that is:

$$\begin{aligned} \eta_1 &= z_1 \\ \eta_2 &= z_2 - \boldsymbol{r}_1\cdot\boldsymbol{\nabla_\xi} z_1 \end{aligned} \tag{5.8}$$

where, again, $\boldsymbol{\nabla_\xi}$ is the horizontal bi-dimensional gradient. We can note from (5.8) that $\boldsymbol{r}_2$ is absent emphasizing that the second-order Eulerian formalism misses all effects related to $\boldsymbol{r}_2$ contribution.

† The factor 1/2 is missing in the original paper by Longuet-Higgins, as was later acknowledged by the author himself

From (4.45), we have at the free surface ($\delta = 0$) :

$$z_2 = \frac{1}{2}\iint \left\{ \left(\frac{k+k'+\Omega^-}{4} - \frac{\sqrt{kk'}||\boldsymbol{k}+\boldsymbol{k}'||}{\Omega^+ - ||\boldsymbol{k}+\boldsymbol{k}'||} \right)(1-\widehat{\boldsymbol{k}}\cdot\widehat{\boldsymbol{k}}')a_{\boldsymbol{k}}a_{\boldsymbol{k}'}\cos(\psi+\psi') + \left(\frac{k+k'+\Omega^+}{4} + \frac{\sqrt{kk'}||\boldsymbol{k}-\boldsymbol{k}'||}{\Omega^- - ||\boldsymbol{k}-\boldsymbol{k}'||} \right)(1+\widehat{\boldsymbol{k}}\cdot\widehat{\boldsymbol{k}}')a_{\boldsymbol{k}}a_{\boldsymbol{k}'}\cos(\psi-\psi') \right\}$$

with $a_{\boldsymbol{k}} = ||A(\boldsymbol{k})||$ and $\psi = \boldsymbol{k}\cdot\boldsymbol{\xi} - \omega t + \varphi_{\boldsymbol{k}}$ where $\varphi_{\boldsymbol{k}}$ is the phase of $A(\boldsymbol{k})$. After some basic algebra we can rewrite z_2 in the form:

$$z_2 = \frac{1}{2}\iint a_{\boldsymbol{k}}a_{\boldsymbol{k}'}\left[K\cos(\psi)\cos(\psi') + \left(K' + \boldsymbol{k}'\cdot\widehat{\boldsymbol{k}} + \boldsymbol{k}\cdot\widehat{\boldsymbol{k}}'\right)\sin(\psi)\sin(\psi')\right] \tag{5.9}$$

where kernels K and K' are the continuous version of kernels K_{ij} and K'_{ij} of (5.7) wherein the indexes i and j are related to non-primed and primed variables.

To complete the expression (5.8) we observe that:

$$\begin{aligned} -\boldsymbol{r}_1\cdot\boldsymbol{\nabla}_{\boldsymbol{\xi}}\eta_1|_{\delta=0} &= -\boldsymbol{\nabla}_{\boldsymbol{\xi}}(\Phi_1)\cdot\boldsymbol{\nabla}_{\boldsymbol{\xi}}(\Phi_{1\delta})|_{\delta=0} \\ &= -\iint (\boldsymbol{k}'\cdot\widehat{\boldsymbol{k}})\; a_{\boldsymbol{k}}a_{\boldsymbol{k}'}\sin(\psi)\sin(\psi') \\ &= -\iint \frac{1}{2}(\boldsymbol{k}'\cdot\widehat{\boldsymbol{k}} + \boldsymbol{k}\cdot\widehat{\boldsymbol{k}}')a_{\boldsymbol{k}}a_{\boldsymbol{k}'}\sin(\psi)\sin(\psi'). \end{aligned} \tag{5.10}$$

The combination of (5.9) and (5.10) yields to:

$$\eta_2 = \frac{1}{2}\iint a_{\boldsymbol{k}}a_{\boldsymbol{k}'}\left[K\cos(\psi)\cos(\psi') + K'\sin(\psi)\sin(\psi')\right], \tag{5.11}$$

which is the continuous version of the equation (5.6) derived by Longuet-Higgins (1963).

5.2. *Consistency with the Lagrangian derivation of W.J. Pierson*

In 1961 W.J. Pierson derived a Lagrangian second-order solution of the discrete long-crested problem. He considered waves traveling in the positive α direction only and found the solutions in the form (equations (27) and (28) in Pierson (1961)):

$$\begin{aligned} x(\alpha,\delta,t) = \alpha &- \sum_i a_i e^{k_i\delta}\sin(\psi_i) - \sum_{j>i}\sum_i \frac{a_i a_j}{g}\left(\frac{\omega_i^3+\omega_j^3}{\omega_j-\omega_i}\right)e^{(k_j+k_i)\delta}\sin(\psi_j-\psi_i) \\ &+ \sum_{j>i}\sum_i \frac{a_i a_j}{g}(\omega_j+\omega_i)\omega_j e^{(k_j-k_i)\delta}\sin(\psi_j-\psi_i) + \sum_i a_i^2\omega_i k_i e^{2k_i\delta}t \end{aligned} \tag{5.12}$$

$$\begin{aligned} z(\alpha,\delta,t) = \delta &+ \sum_i a_i e^{k_i\delta}\cos(\psi_i) + \sum_{j>i}\sum_i \frac{a_i a_j}{g}\left(\omega_i^2+\omega_i\omega_j+\omega_j^2\right)e^{(k_j+k_i)\delta}\cos(\psi_j-\psi_i) \\ &- \sum_{j>i}\sum_i \frac{a_i a_j}{g}(\omega_j+\omega_i)\omega_j e^{(k_j-k_i)\delta}\cos(\psi_j-\psi_i) \end{aligned} \tag{5.13}$$

$$\begin{aligned} p(\alpha,\delta,t) = p_a - \rho g\delta &+ \rho g\sum_i \frac{a_i^2 k_i}{2}\left(e^{2k_i\delta}-1\right) - 2\rho\sum_{j>i}\sum_i a_i a_j\omega_i\omega_j e^{(k_j+k_i)\delta}\cos(\psi_j-\psi_i) \\ &+ 2\rho\sum_{j>i}\sum_i a_i a_j\omega_i\omega_j e^{(k_j-k_i)\delta}\cos(\psi_j-\psi_i) \end{aligned} \tag{5.14}$$

with $\psi_i = k_i\alpha - \omega_i t + \varphi_i$.

The comparison of our continuous solution with the discrete formulation of Pierson is not straightforward due to the principal value formulation of one of the terms. However, we can note that within a small subspace $\mathcal{D}$ of $\Re^4$ around the singularity domain ($|\omega - \omega'| < \varepsilon$) we have:

$$PV \iint_{\mathcal{D}} i \left(\frac{\omega \boldsymbol{k} + \omega' \boldsymbol{k'}}{2(\omega - \omega')} e^{(k+k')\delta} e^{-i(\omega-\omega')t} \right) \underline{\mathcal{B}} + c.c. \simeq \iint_{\mathcal{D}} \tfrac{1}{2} \omega k (\widehat{\boldsymbol{k}} + \widehat{\boldsymbol{k}}') e^{(k+k')\delta} \underline{\mathcal{B}}\ t \quad (5.15)$$

This result corresponds to a temporal secular term. More detailed comments on this term can be found in section 6.1.

Moreover, we can note that (see equation (4.38)):

$$\underline{\boldsymbol{\mathcal{R}'}} \xrightarrow[\boldsymbol{k} \to \boldsymbol{k'}]{} k(\widehat{\widehat{\boldsymbol{k}} - \widehat{\boldsymbol{k}}'}) \quad (5.16)$$

Within a small subspace $\mathcal{D}'$ of $\Re^4$ defined by $||\boldsymbol{k} - \boldsymbol{k}'|| < \varepsilon$ and due to the symmetry of the previous limit we have:

$$\iint_{\mathcal{D}'} i \frac{\sqrt{kk'}(\boldsymbol{k} - \boldsymbol{k}')}{\Omega^- - ||\boldsymbol{k} - \boldsymbol{k}'||} e^{||\boldsymbol{k} - \boldsymbol{k}'||\delta} \underline{\mathcal{B}} e^{-i(\omega - \omega')t} + c.c \xrightarrow[\epsilon \to 0]{} 0 \quad (5.17)$$

since integration is realized over all $\boldsymbol{k}$ and $\boldsymbol{k}'$.

Restricting solution (4.45) to the discrete case of long-crested waves traveling in the same positive α direction ($\widehat{\boldsymbol{k}} \cdot \widehat{\boldsymbol{k}}' = 1$, $||\boldsymbol{k} - \boldsymbol{k}'|| = s(k - k')$ where s is the sign of $k - k'$) we obtain the following expressions for the second-order displacements and pressure:

$$\begin{aligned}
x_2 &= -\sum_{\substack{i,j \\ i \neq j}} \left[\frac{\omega_i k_i + \omega_j k_j}{2(\omega_i - \omega_j)} e^{(k_i + k_j)\delta} + \frac{\sqrt{k_i k_j}(k_i - k_j)}{\Omega_{ij}^- - s(k_i - k_j)} e^{s(k_i - k_j)\delta} \right] a_i a_j \sin(\psi_i - \psi_j) \\
&\quad + \sum_i a_i^2 \omega_i k_i e^{2k_i \delta} t \\
z_2 &= \sum_{i,j} \left[\frac{k_i + k_j + \Omega_{ij}^+}{4} e^{(k_i + k_j)\delta} + \frac{\sqrt{k_i k_j} s(k_i - k_j)}{\Omega_{ij}^- - s(k_i - k_j)} e^{s(k_i - k_j)\delta} \right] a_i a_j \cos(\psi_i - \psi_j) \\
p_2 &= -\rho g \sum_{i,j} \sqrt{k_i k_j} \left(e^{(k_i + k_j)\delta} - e^{s(k_i - k_j)\delta} \right) a_i a_j \cos(\psi_i - \psi_j) \quad (5.18)
\end{aligned}$$

where non-primed and primed variables of (4.45) are related to the indexes i and j, respectively. Making use of the dispersion relationship $\omega^2 = gk$ we can rewrite after straightforward manipulations:

$$
\begin{aligned}
x_2 =& -\sum_{j>i}\sum_{i} \frac{a_i a_j}{g}\left(\frac{\omega_i^3+\omega_j^3}{\omega_j-\omega_i}\right) e^{(k_j+k_i)\delta}\sin(\psi_j-\psi_i) \\
&+\sum_{j>i}\sum_{i}\frac{a_i a_j}{g}(\omega_j+\omega_i)\omega_j e^{(k_j-k_i)\delta}\sin(\psi_j-\psi_i)+\sum_i a_i^2\omega_i k_i e^{2k_i\delta}t \qquad (5.19)\\
z_2 =& \sum_{j>i}\sum_{i}\frac{a_i a_j}{g}\left(\omega_i^2+\omega_i\omega_j+\omega_j^2\right)e^{(k_j+k_i)\delta}\cos(\psi_j-\psi_i)\\
&-\sum_{j>i}\sum_{i}\frac{a_i a_j}{g}(\omega_j+\omega_i)\omega_j e^{(k_j-k_i)\delta}\cos(\psi_j-\psi_i)+\sum_i \tfrac{1}{2}a_i^2 k_i e^{2k_i\delta} \qquad (5.20)\\
p_2 =& \rho g\sum_i \frac{a_i^2 k_i}{2}\left(e^{2k_i\delta}-1\right)-2\rho\sum_{j>i}\sum_i a_i a_j\omega_i\omega_j e^{(k_j+k_i)\delta}\cos(\psi_j-\psi_i)\\
&+2\rho\sum_{j>i}\sum_i a_i a_j\omega_i\omega_j e^{(k_j-k_i)\delta}\cos(\psi_j-\psi_i) \qquad (5.21)
\end{aligned}
$$

which differs from the original derivation by Pierson (5.12)-(5.14) by the constant term $\sum_i \frac{1}{2}a_i^2 k_i e^{2k_i\delta}$ in the vertical displacement corresponding to the mean of z_2. A closer inspection of Pierson (1961) original derivation shows that he used $\partial|\mathbb{J}|/\partial t = 0$ as its basic continuity equation. However, this does not necessarily implies $|\mathbb{J}| = 1$ and can lead to erroneous solutions. Using equation $\partial|\mathbb{J}|/\partial t = 0$ instead of $|\mathbb{J}| = 1$ allows the cancellation of all the time-independent terms in the solutions. This is the reason why the mean level of z_2 is absent in Pierson (1961) derivations which must be rectified as equations (5.19)-(5.21).

6. Second-order inspection

6.1. *Stokes drift*

We will now investigate some remarkable properties of the second-order Lagrangian solution. The first one is the customary Stokes drift, first introduced in the celebrated work by Stokes (1847) and extended to the tri-dimensional case by Kenyon (1969) and Phillips (1977). The Stokes drift manifests in a net horizontal displacement after one wave period or, more generally, after time averaging. The net mass transport can be evaluated using the horizontal velocity $\boldsymbol{r}_{2t}$ estimation. As shown in the derivation below, only the third integral term $\underline{\boldsymbol{r}}_2$ (see equation (4.40)) in the expression of $\boldsymbol{r}_2$ has a non-vanishing temporal mean. Equation (6.1) gives the horizontal velocity for this term only (note that the apparent singularity disappears after differentiation).

$$\underline{\boldsymbol{r}}_{2t} = \iint \tfrac{1}{2}(\omega\boldsymbol{k}+\omega'\boldsymbol{k}')e^{(k+k')\delta}\underline{\mathcal{B}}e^{-i(\omega-\omega')t} + c.c. \qquad (6.1)$$

We now consider the time average of this quantity:

$$\langle\underline{\boldsymbol{r}}_{2t}\rangle_t = \lim_{T\to\infty}\frac{1}{T}\int_{-T/2}^{T/2}dt\iint_{\Re^4}\tfrac{1}{2}(\omega\boldsymbol{k}+\omega'\boldsymbol{k}')\underline{\mathcal{B}}e^{-i(\omega-\omega')t}e^{(k+k')\delta} + c.c. \qquad (6.2)$$

Inverting time and space integrals and using:

$$\lim_{T\to\infty}\frac{1}{T}\int_{-T/2}^{T/2}\cos\left[(\omega-\omega')t\right]dt = \eth(\omega-\omega') \qquad (6.3)$$

where $\eth$ is the Dirac distribution, we obtain:

$$\langle \boldsymbol{r}_{2t} \rangle_t = \iint\limits_{\Re^4} \eth(\omega - \omega') \tfrac{1}{2} \omega k (\widehat{\boldsymbol{k}} + \widehat{\boldsymbol{k}}') \underline{\mathcal{B}} e^{2k\delta} + c.c. \tag{6.4}$$

All other terms in $\boldsymbol{r}_{2t}$ have a vanishing temporal mean due to their $\omega - \omega'$ dependency which appears after temporal differentiation and due to the Dirac function. This is why $\underline{\boldsymbol{r}}_{2t}$ is replaced by $\boldsymbol{r}_{2t}$ in equation (6.4). Equation (6.4) is thus the total mean average of particles horizontal displacement. Using again (6.3) in the space domain, we derive the spatial mean of (6.4) which writes:

$$\langle \boldsymbol{r}_{2t} \rangle_{\boldsymbol{\xi} t} = \iint\limits_{\Re^4} \eth(\omega - \omega') \eth(\widehat{\boldsymbol{k}} - \widehat{\boldsymbol{k}}') \tfrac{1}{2} \omega k (\widehat{\boldsymbol{k}} + \widehat{\boldsymbol{k}}') \tfrac{1}{4} (1 + \widehat{\boldsymbol{k}} \cdot \widehat{\boldsymbol{k}}') A(\boldsymbol{k}) A^*(\boldsymbol{k}') e^{2k\delta} + c.c. \tag{6.5}$$

Simplified as:

$$\langle \boldsymbol{r}_{2t} \rangle_{\boldsymbol{\xi} t} = \int \omega \boldsymbol{k} ||A(\boldsymbol{k})||^2 e^{2k\delta} \tag{6.6}$$

we easily identify the classical Stokes drift velocity. The mean Stokes drift $\langle \boldsymbol{r}_2 \rangle_{\boldsymbol{\xi} t}$ is thus already included as a part of $\boldsymbol{r}_2$ expression (4.45) and is the results of the self-interaction of the different harmonics. Clamond (2007) derived this result for a monochromatic wave and noted that after subtraction of this mass transport component, the orbits of water particles remain closed and symmetric even for steep waves (see also Longuet-Higgins (1987)). As noted before in section 5.1 equation (5.8), the contribution of $\boldsymbol{r}_2$ is absent in the Eulerian expansion leading to the absence of the Stokes drift in the second order Eulerian expansion.

6.2. *Horse-shoe patterns*

In the case of tri-dimensional multiple wave interactions, a residual spatial Stokes drift pattern, namely $\langle \boldsymbol{r}_{2t} \rangle_t - \langle \boldsymbol{r}_{2t} \rangle_{\boldsymbol{\xi} t}$, remains. It results from the interaction of harmonics having the same time frequency but different propagation directions. This phenomena which cannot exist in the bi-dimensional case (because $\omega = \omega'$ implies $k = k'$) is responsible for the increase of the wave shape asymmetry with time. An example is shown on Figure 1. Two harmonics with the same frequency but propagating in different directions create a spatially varying shear over the sea surface (figure 1(b)). This shear tends to slow down the troughs relatively to the crests leading to an asymmetric wave shape that can be related to the first stage of the formation of the well-known horse shoe patterns (see figure 1(c)). It nevertheless preserves the front back symmetry of the waves and no slope skewness.

Shrira *et al.* (1996) and later Annenkov & Shrira (1999) proposed a mathematical solution to explain the apparition and the persistence of the horse shoe pattern by quintet resonant interactions coupled with wind and dissipation and noted that they develop front-back asymmetries. However, horse shoe patterns can be generated even in the absence of wind (e.g. Su *et al.* (1982)) which means that nonlinear interactions of gravity waves can account for their existence. In any case, two main characteristics of the horse-shoe patterns are a) a life time largely exceeding the associated wave period and b) a persistent shape with front-back asymmetry.

For clarity, in the explanations below, the term *harmonic* is used for a Lagrangian wave vector component and the term *wave* is used for an Eulerian (surface) wave vector component. Even though it does not seem easy to cross-compare harmonic-interactions and wave-interactions we can try to guess which harmonics are involved in such horse-shoe pattern. Bi-harmonic interactions terms are present in both horizontal (x_2, y_2) and

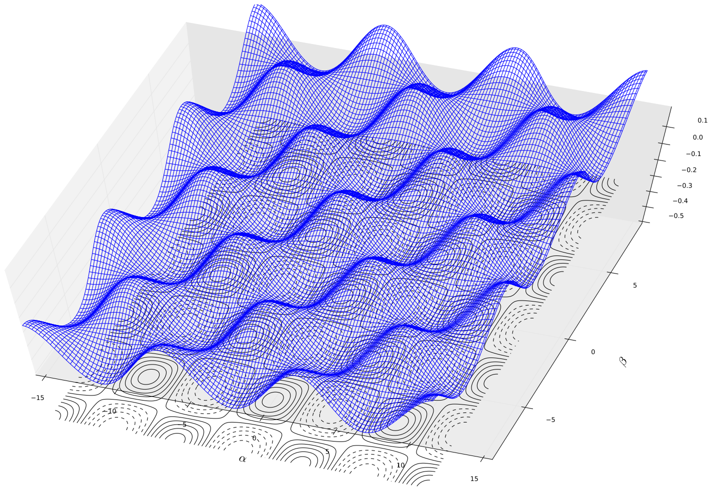

(a) Sea surface elevation at $t = 0$.

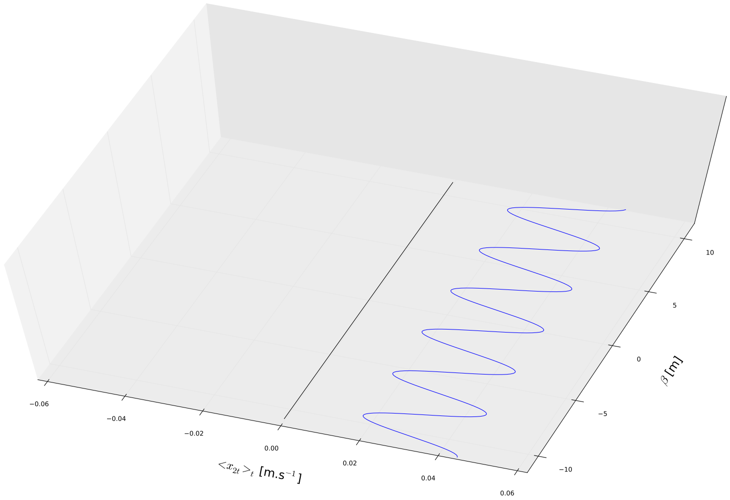

(b) α component of the Stokes drift velocity: $\langle \boldsymbol{r}_{2t} \rangle_t$ (β component vanish). It is independent of α. We can see a mean Stokes drift of about 3 cm.s^{-1} and its spatial variations leading to increasing crescent shape patterns.

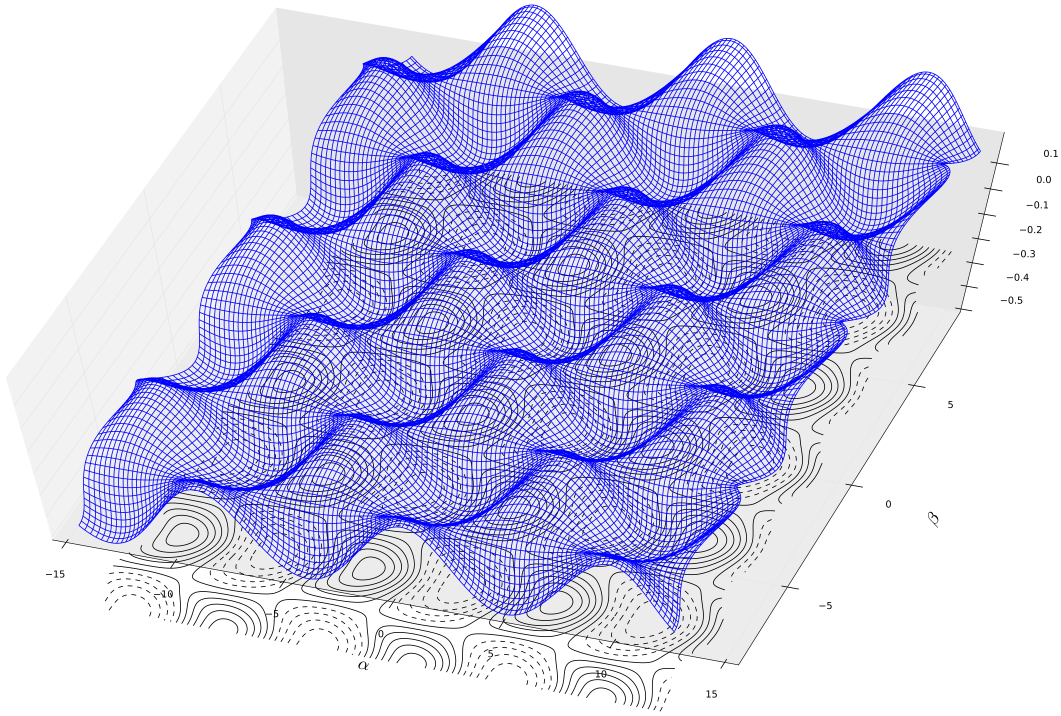

(c) Sea surface elevation after a large time lag of 30 seconds. Surface has developed horse shoe patterns.

Figure 1. Interaction of two harmonics with same amplitudes ($A = 0.08$ m) and wavenumbers ($k = 1.104$ rad.m^{-1}) with different directions of propagation: + and − 48.2 degrees relative to α direction.

vertical (z_2) second order Lagrangian displacements. Thus, four-waves interactions in the Eulerian framework should be *a priori* available, at least partially, with bi-harmonic Lagrangian interactions only. Horse-shoe patterns observed by Collard & Caulliez (1999) presents peculiar features that can be compared with the presented model. Their experiment starts from an almost monochromatic wave with wavenumber $\boldsymbol{k}_0$. Then, the wave field degenerate and gives rise to crescent shape patterns. Their spatiotemporal analysis shows that a pair of harmonics $(\boldsymbol{k}_1, \boldsymbol{k}_2)$ are created such as :

$$\boldsymbol{k}_1 + \boldsymbol{k}_2 = 3\boldsymbol{k}_0 \quad \text{and} \quad \omega_1 + \omega_2 = 3\omega_0 \tag{6.7}$$

The case called "steady pattern" in Collard & Caulliez (1999) is defined with $k_1 = k_2$ and consequently $\omega_1 = \omega_2$. In that specific case, the results presented on figure 1 suggests that no $\boldsymbol{k}_0$ component is necessary to obtain horse-shoe patterns since the secular term in $\langle \boldsymbol{r}_{2t} \rangle_t - \langle \boldsymbol{r}_{2t} \rangle_{\boldsymbol{\xi} t}$ is generated by the $\boldsymbol{k}_1$ and $\boldsymbol{k}_2$ component interaction only. However, since the $\boldsymbol{k}_0$ component is obviously present in Collard & Caulliez (1999) experiment, it was not experimentally possible to check its necessity for the horse-shoe generation. Yet, we could invoke that it was indirectly necessary to give rise to the perfectly symmetric pair of wave vector $(\boldsymbol{k}_1, \boldsymbol{k}_2)$ through the resonant interaction defined by equation (6.7). It should thus be interesting to experimentally show that a unique bi-harmonic structure such as presented in figure 1 is sufficient to create horse-shoe patterns.

However, for comparison purposes, we added a $\boldsymbol{k}_0$ component in the orbital spectrum used in the simulation presented on figure 1 chosen such as $\boldsymbol{k}_1 + \boldsymbol{k}_2 = 3\boldsymbol{k}_0$, $\varphi_0 = -\pi/2$ and $\varphi_1 = \varphi_2 = 0$ (but obviously $\omega_1 + \omega_2 \neq 3\omega_0$). We were capable to reproduce the "steady" horse-shoe patterns presented in Collard & Caulliez (1999). Figure 2(a) shows the wave field obtained after 30 seconds and figures 2(b) and 2(c) show the temporal record of the water surface elevation and its Fourier transform. As pointed out by Collard & Caulliez (1999), it contains a $\frac{3}{2}\omega_0$ harmonic (0.524 Hz) coming from the simple first order contribution of $\boldsymbol{k}_1$ and $\boldsymbol{k}_2$. We believe that the front-back asymmetry observed in real conditions in the horse-shoe pattern comes from higher-order interaction (Lagrangian cubic order) that would create a $\boldsymbol{k}_0$ component with an angular frequency of ω_0 but with a slightly different phase.

In any case, even if the spatial drift we have found tends to slowly twist the wave shape and let it tend to the horse-shoe pattern, it leads to a constant increase of the surface deformation with time giving rise to unrealistic shape at large time lags. Moreover, as already noted by Shrira *et al.* (1996), steady wave solutions of inviscid equations do not present front back asymmetries. Hence, the secular term can only belong to a transitory state of the surface and cannot be used for large time lags as suggested by the domain of validity of the series expansion. As already mentioned, the Stokes drift manifests itself through a secular term which is undesirable in a perturbation expansion. Indeed, as commented by Buldakov *et al.* (2006), third order solutions will make the secular term interact with the leading order creating unrealistic diverging secular terms in both horizontal and vertical particles expansion. As a result, the second-order solution cannot be valid at arbitrary large time. Furthermore, any attempt to pursue the Lagrangian expansion beyond the order two should be accompanied with a particles relabeling as suggested by Clamond (2007). He indeed claimed that a steady solution with Stokes drift cannot be found without adapting the Lagrangian references. The apparition of the mean secular term in a Lagrangian expansion comes from a misrepresentation of steady waves and can be avoided, at least for a monochromatic wave, by a correct time and space dependent water particles relabeling leading to a valid solution at all time and orders. However, as this paper deals with tri-dimensional multiple wave system and is

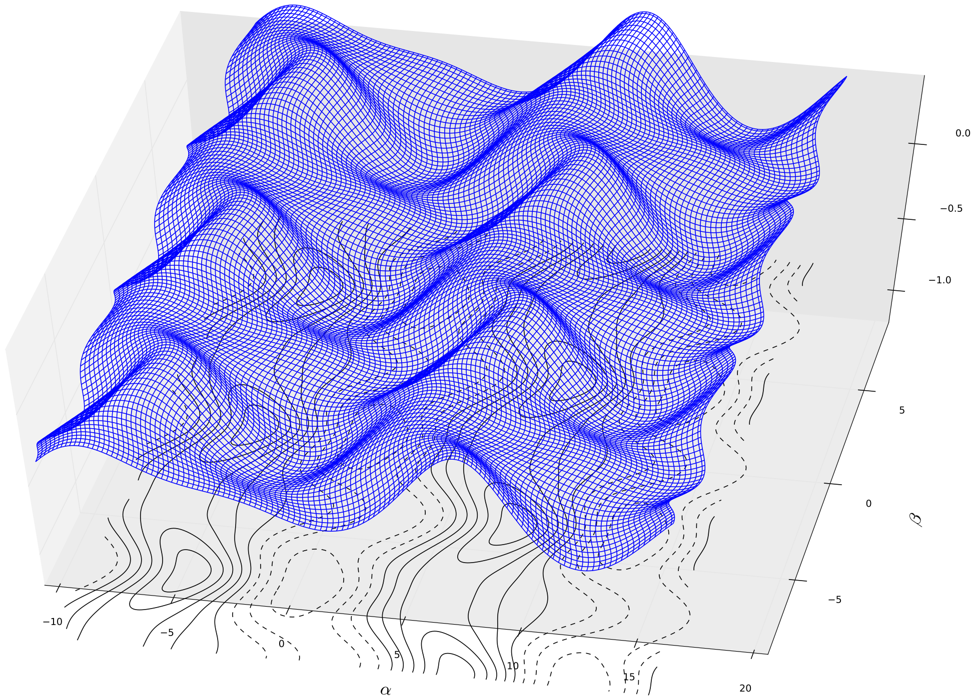

(a) Sea surface elevation at $t = 30$ s.

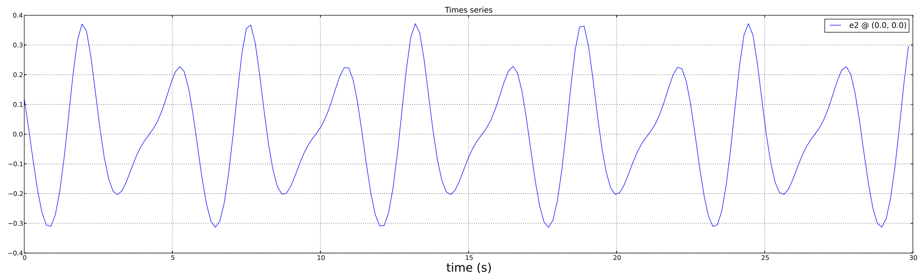

(b) Temporal record of the water surface elevation at fixed point $(\alpha, \beta) = (0, 0)$

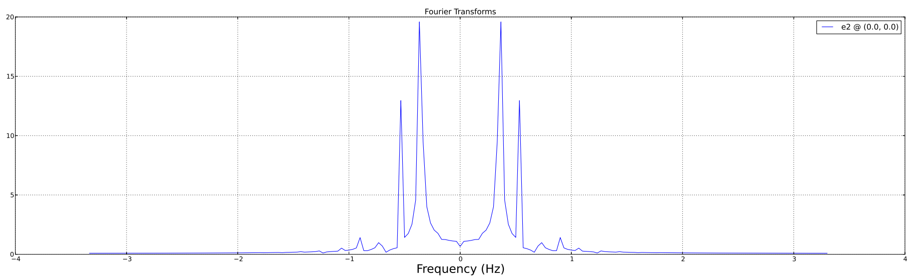

(c) Fourier Transform of the temporal record (figure 2(b)). We can identify frequency $f_0 = (2\pi)^{-1}\sqrt{gk_0}$ and harmonic $\frac{3}{2}f_0$ coming for $\boldsymbol{k}_1$ and $\boldsymbol{k}_2$ contribution.

FIGURE 2. Surface elevation obtained with three harmonics: $k_0 = 0.491$ rad.m^{-1}, $k_1 = k_2 = 1.104$ rad.m^{-1}, respective amplitudes: $a_0 = 0.24$ m and $a_1 = a_2 = 0.06$ m, directions of propagation relative to α: $\theta_0 = 0, \theta_1 = -\theta_2 = \arccos(\frac{2}{3})$ and phases $\varphi_0 = -\frac{\pi}{2}, \varphi_1 = \varphi_2 = 0$.

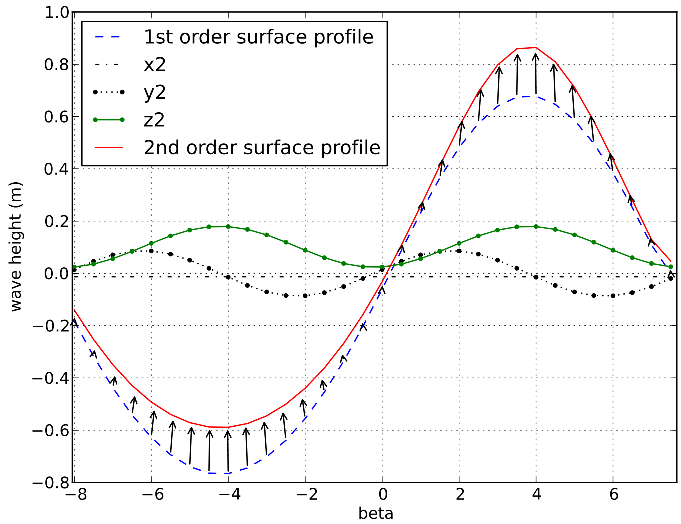

FIGURE 3. Slices along an equi-α contour (perpendicular to the mean direction of wave) of the first- and second-order Lagrangian surface. The slices pass through a wave crest. The different second-order contributions are superimposed as well as their combined effects (arrows).

restricted to the second-order expansion, we will not enter into such details and leave these considerations for further studies.

6.3. *Sharp crests, mean elevation and skewness coefficient*

For the temporal mean of the second-order vertical displacement at the surface we have:

$$\langle z_2 \rangle_{t,\ \delta=0} = \iint_{\Re^4} \eth(\omega - \omega')\tfrac{1}{2}k\underline{\mathcal{B}} + c.c. \tag{6.8}$$

This shows that the second-order vertical displacement has a non-vanishing mean due to the interaction of waves with the same frequency. The $(\widehat{\boldsymbol{k}} - \widehat{\boldsymbol{k}}')$ phase term in $\underline{\mathcal{B}}$ describes a spatial oscillating pattern perpendicular to the mean direction of wave and is the main contributor to the vertical second-order displacement. To illustrate this statement, we use the same bi-harmonic system as described above. Figure 3 displays first- and second-order surface slices along an equi-α contour corresponding to a crest position. As can be plainly seen, the second-order vertical term tends to permanently sharpen the crests and flatten the troughs by a positive vertical shift relative to z_2 mean level. Contrarily to the Lagrangian first-order terms, the sharpening and flattening effects apply in the direction perpendicular to the wave direction leading to a more “short-crested” wave pattern. The horizontal term y_2 has the same effect even though it is in quadrature with the vertical motion. The combination of the two effects is represented with arrows on Figure 3.

It was shown by Pierson (1961) equation (45) that the first order Lagrangian surface has a relative mean level :

$$\overline{\eta}_1 = -\int k||A(\boldsymbol{k})||^2 \tag{6.9}$$

The mean sea level is affected by the non-vanishing mean of the second-order elevation term (see mean level of z_2 on figure 3). At the surface :

$$\langle z_2 \rangle_{\boldsymbol{\xi},t} = \int \tfrac{1}{2} k ||A(\boldsymbol{k})||^2 \tag{6.10}$$

is the unique second order contributor to the mean surface elevation at the leading order giving the global sea level:

$$\overline{\eta}_2 = -\int \tfrac{1}{2} k ||A(\boldsymbol{k})||^2 \tag{6.11}$$

When this mean level is naturally tared by a Lagrangian sensor (free-floating buoys, ...), it gives a greater mean sea level than an Eulerian measuring system (fixed probes, ...) by the amount of $|\overline{\eta}_2|$. This conclusion was already raised by Longuet-Higgins (1986) (see equation (3.7)) via a different route. He emphasized its importance in particular for ocean surface remote sensing applications. However, as already stated by Longuet-Higgins (1987), Lagrangian orbits are highly symmetric to the second order leading to a vanishing skewness. In random ocean wave fields, such second-order dynamical effects have strong impacts on waves height, slope and curvature distributions and are responsible for their deviation from the Gaussian law. These statistical properties are of great interest in the ocean remote sensing community but a systematic study goes beyond the scope of this paper and is left for further developments.

6.4. *Modulational Benjamin-Feir instability, a simple beat effect*

It is now well known that Benjamin & Feir (1967) (BF) instability results from a nonlinear quartet-wave resonant phenomenon. An initial uniform monochromatic Stokes wave of moderate amplitude degenerates and develops side-band harmonics with an exponential rate of growth. This phenomenon is usually acknowledged as the first main contributor to the spreading of the spectrum energy. Due to an asymmetric evolution of the two side-band harmonics (when aligned with the carrier wave) induced by an unequal dissipation, the BF instability is one of the indirect contributors of the well-known frequency down-shift (Lake *et al.* (1977); Hara & Mei (1991)). A large number of studies have been dedicated to this phenomenon and we refer to Dias & Kharif (1999) for an exhaustive bibliography on the subject. Zakharov (1968) has shown that this phenomenon appears at third order with respect to the non-linearity parameter of the Zakharov equations which are developed in an Eulerian framework.

Recent analytical and experimental studies (e.g. Shemer (2010); Segur *et al.* (2005)) have shown that an initially monochromatic carrier wave is periodically and alternatively exchanging energy with its two side-band harmonics. The latter are rapidly generated at the beginning of the propagation and their exponential growth coefficient is controlled by the carrier characteristics. As rigorously shown by Segur *et al.* (2005) with the Schrödinger equations, the temporal limit of the exponential period of growth of sideband harmonics can be explained by a damping coefficient that limits the growth of the perturbations. In the absence of this damping coefficient, the apparition of stronger nonlinear interactions (up to breaking) is responsible of the limited growth. In both cases, after a short limited period of growth, a stabilized regime of modulation-demodulation is established.

In this section we do not wish to enter into a complex analytical analysis but would like to show, on the basis of theoretical and numerical considerations, that the periodic regime of BF instability is already present (at least partly) and symmetric (i.e with no frequency down-shift) in the Lagrangian second-order solution.

We do not study the period of growth since we only look at periodic solutions but we show that, at second order in the nonlinear Lagrangian parameter, a periodic modula-

k	$k_2 - k_0$	$2k_0 - k_2$	k_0	k_2	$2k_2 - k_0$
$\lvert A(k)\rvert$	0	0	0.2228	0.0178	0
$\lvert\hat{x}(k)\rvert$	0.2785	0	0.2228	0.0178	0
$\lvert\hat{z}(k)\rvert$	0.0062	0	0.2228	0.0178	0
$\lvert\hat{\eta}(k)\rvert$	0.0018	**0.04627**	0.1979	0.0598	0.0093

TABLE 1. Orbital $|A(k)|$, horizontal $|\hat{x}|$, vertical $|\hat{z}|$ motions and surface $|\hat{\eta}|$ spectral amplitudes obtained from a two-wave orbital system : $(k_0,\ k_2) = \pi/2\times(1,\ 1{+}p)$ and $(a_0,\ a_2) = s/k_0\times(1,\ c)$ with $s = 0.35$, $p = 0.1$ and $c = 0.08$.

tion process exists between the carrier and two existing sideband harmonics and can be interpreted as a Lagrangian Benjamin-Feir modulation. We show that, surprisingly, what is considered as a periodical exchange of energy between waves in an Eulerian point of view is in fact a simple beat effect which appears naturally when a two-wave system has close frequencies in the Lagrangian framework. The same initial sea state is used in the Eulerian framework and show that this phenomenon is clearly absent up to the second order.

6.4.1. *System of three aligned harmonics*

In order to illustrate this statement, we consider a bi-dimensional and unidirectional case defined up to the second-order by equations (5.12)-(5.13). We focus on a bi-harmonics system defined by its wavenumbers k_0 and k_2 ($0 < k_0 < k_2$) where k_0 is the carrier wavenumber, k_2 the satellite wavenumber and φ_0 and φ_2 their respective phases. The carrier wave is chosen with wavenumber $k_0 = \pi/2$ rad.m^{-1} propagating in the α direction and corresponding to a 4 m wavelength and a 1.6 s time period. Its orbital amplitude $a_0 = 0.2228$ m is chosen such as $s = k_0 a_0 = 0.35$. It must however be emphasized that a_0 is the orbital spectral amplitude and that the real amplitude of the carrier never exceed 0.2 m leading to a maximum steepness of 0.3. The satellite wavenumber is $k_2 = k_0\times(1{+}p)$ with $p = 0.1$. Its orbital amplitude is $a_2 = a_0 \times c$ with $c = 0.08$.

We generate a 90 m length surface with a 12.5 cm label spatial sampling over a thousand periods of the carrier wave and evaluate, at each time step, the spectral amplitude of the surface $\eta(\alpha,\ t)$ (a numerical interpolation of the surface profile on a regular grid was realized prior to its Fourier Transform), the horizontal $x(\alpha,\ t)$ and vertical $z(\alpha,\ t)$ particle displacement processes at the surface $\delta = 0$. We therefore evaluate the Fourier Transforms $\hat{\eta}(k,\ t)$, $\hat{x}(k,\ t)$ and $\hat{z}(k,\ t)$ defined by:

$$\hat{\Psi}(k,t) = \int (\Psi(\alpha,t) - \overline{\Psi})e^{ik\alpha}d\alpha, \tag{6.12}$$

where Ψ stands for any of the three quantities η, x or z and where the upper line $\overline{\Psi}$ refers to the spatial average. These quantities are constant in time and are given on Table 1 together with the orbital spectral amplitudes $|A(k)|$. We have selected the wavenumbers associated to non-vanishing amplitudes. All harmonics of the orbital spectrum are aligned and produce a unique temporal secular term corresponding to a global horizontal translation of the sea surface profile. This main constant drift can easily be removed by adapting the frame of reference ensuring the validity of the second order expansion, in this case only, even for large time lag.

Even though neither the vertical ($|\hat{z}|$) or horizontal ($|\hat{x}|$) displacement spectra contain a $2k_0 - k_2$ component, the surface does. The $k_2 - k_0$ component is important contributor

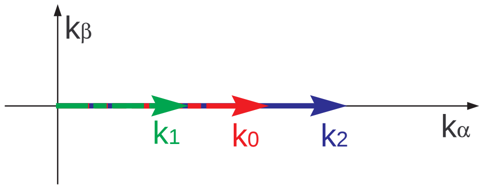

FIGURE 4. Spectral repartition of the orbital spectrum components. $k_1 + k_2 = 2k_0$

to the second-order horizontal displacement:

$$-\frac{a_0 a_2}{g}\left(\frac{\omega_0^3+\omega_2^3}{\omega_2-\omega_0}\right)\sin\left[(k_2-k_0)x-(\omega_2-\omega_0)t+\varphi_2-\varphi_0\right] \tag{6.13}$$

Table 1 clearly shows a $k_0 - (k_2 - k_0) = 2k_0 - k_2$ harmonic in the surface spectra due to the combination of the horizontal $k_2 - k_0$ term and the k_0 one. We can thus easily deduce that the angular frequency and phase of this term write $2\omega_0 - \omega_2$ and $2\varphi_0 - \varphi_2$. The other interaction term with wavenumber $k_0 + (k_2 - k_0) = k_2$ have the same frequency ω_2 and phase φ_2 than the orbital first-order k_2 component of the orbital spectrum and simply affects its amplitude. The case presented on Table 1 shows that the k_2 component of the surface (0.0598) is permanently increased relative to the orbital spectrum (0.0178). The same effect is visible on the $k_2 - (k_2 - k_0) = k_0$ component, leading to a small decrease of the carrier amplitude relative to the orbital spectrum. As expected, the surface spectrum also contains a very small $2k_2 - k_0$ term arising from the combination term $k_2 + (k_2 - k_0)$.

Now, let us suppose that an extra k_1 component is added to the orbital spectrum in such a way that $k_1 = 2k_0 - k_2$ as shown on figure 4 and denote ω_1 and φ_1 as the associated angular frequency and phase. This component will thus have the same spatial wavenumber than the $k_0 - (k_2 - k_0)$ term presented above with a slightly different temporal frequency. These two terms will thus generate a temporal beat effect with angular frequency $\Delta\omega$ such as:

$$\Delta\omega = \omega_1 - (2\omega_0 - \omega_2) \tag{6.14}$$

and the phase of k_1 amplitude temporal evolution will thus only depends on the global phase:

$$\theta = \varphi_1 - (2\varphi_0 - \varphi_2). \tag{6.15}$$

Inverting k_1 and k_2 in the previous considerations we obtain the same behavior for the k_2 component. Now, letting the tri-harmonics structure system evolve in time leads to a periodical evolution of the two side band harmonic amplitudes with the same period :

$$T = \frac{2\pi}{\Delta\omega} \tag{6.16}$$

and the same evolution phase depending on the unique value θ. The time evolution of the carrier, high frequency (HF) and low frequency (LF) side-band amplitudes is presented on Figure 5. The corresponding Eulerian case is presented for comparison purposes and clearly shows that the Benjamin Feir modulation is absent up to the second order. Shemer (2010) already derived these two results with a different technique in the Eulerian framework by pushing the non-linearity at order three and considering quartet interaction of waves.

It should be noted that the mean level and the variations of a satellite amplitude are not fully controlled by the ratio $c = a_2/a_0$ and depends on the carrier charac-

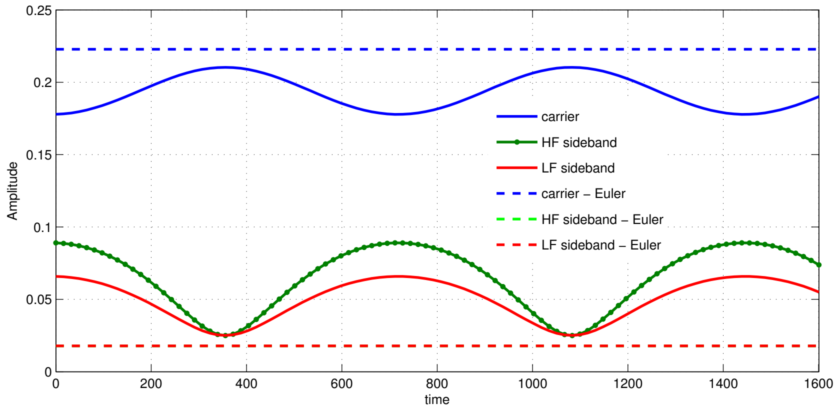

FIGURE 5. Time evolution of the spectral amplitudes of the carrier wave ($\omega_0 = 3.93$ rad.s^{-1}), the Low and High Frequency sidebands ($\omega_1 = 3.74$ and $\omega_2 = 4.11$ rad.s^{-1}). Solid lines are for the Lagrangian expansion and dashed ones for the Eulerian expansion. Period defined equation (6.16) is 726 s.

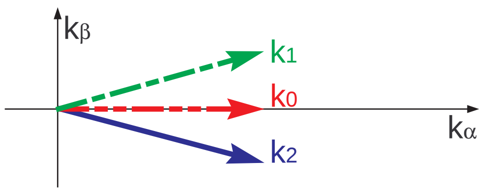

FIGURE 6. Spectral repartition of the orbital spectrum components. $\boldsymbol{k}_1 + \boldsymbol{k}_2 = 2\boldsymbol{k}_0$

teristics and the other satellite. This makes the quantitative comparison between the two approaches complicated. However, it does not change the conclusion that a strong modulation-demodulation of the carrier wave and the two satellites is present at second order in the Lagrangian framework while the Eulerian one does not show any interaction even if the sea surface spectrum present new harmonics relative to the first order.

6.4.2. *Carrier harmonic with two lateral side-bands harmonics*

Let us now consider a symmetric tri-harmonics structure such as $2\boldsymbol{k}_0 = \boldsymbol{k}_1 + \boldsymbol{k}_2$ with $\omega_1 - \omega_0 > 0$ and $\omega_2 - \omega_0 > 0$. This configuration is possible in the 3-dimensional case only and is represented on figure 6. Figure 7 show surfaces profile derived with second-order solutions of the Eulerian (Longuet-Higgins (1963)) and Lagrangian (equation (2.7)) expansion with (3.7) and (4.45) with the same three harmonics structure. The carrier wave is chosen with amplitude $a_0 = 0.2$ m and propagates in the α direction with wavenumber $k_0 = 1.58$ rad.m^{-1} corresponding to a 3.97 m wavelength and a 1.58 s time period. Two satellites of same amplitude $a_1 = a_2 = 0.04$ m with wavenumbers $k_1 = k_2 = k_0/[\cos(37.08°)]$ rad.m^{-1} propagate with angles $+37.08°$ and $-37.08°$ relative to the α direction. Phases of the three harmonics are set to zero. Spatial sampling is 25 cm.

We generate a 8 m $\times$ 8 m surface with a 25 cm spatial sampling over ten periods of the carrier wave and a time evolution process is realized by increasing the time variable. A bi-dimensional spectral analysis of the surfaces is realized at each time step by Fast Fourier

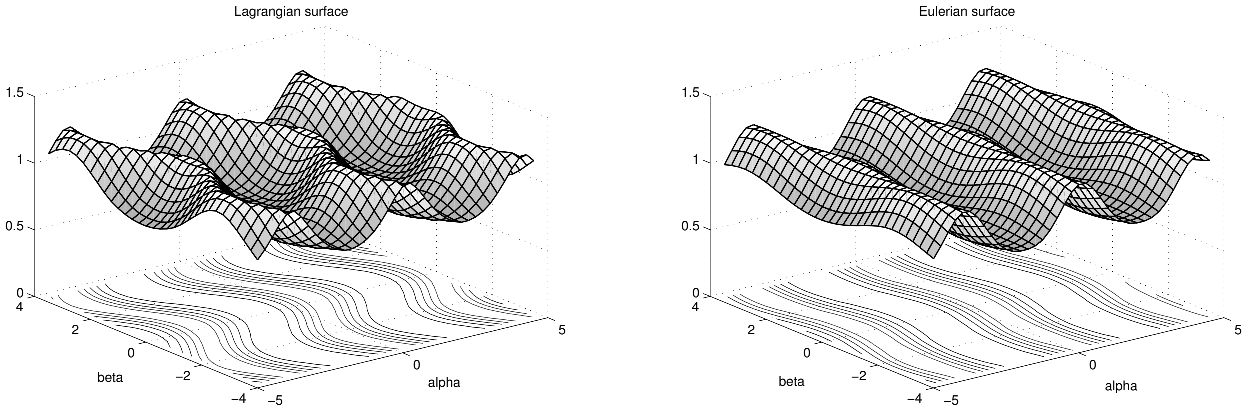

FIGURE 7. Sea surfaces profiles derived from second-order solutions of Lagrangian and Eulerian expansion. $t = 17$ s.

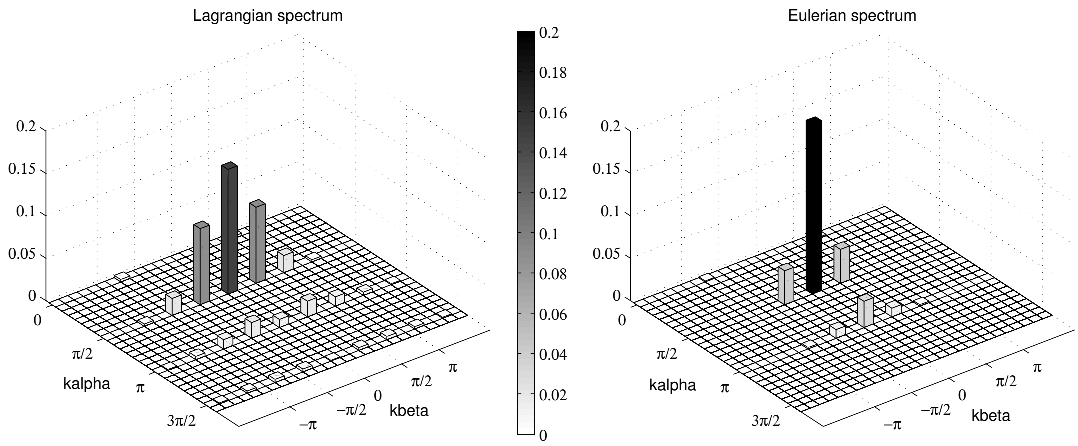

FIGURE 8. Eulerian and Lagrangian surfaces spectra. $t = 17$ s.

Transform. Again, a numerical interpolation of the Lagrangian surface on a regular grid is realized prior to the Fourier Transform. Figure 8 shows the surfaces spectra obtained at $t = 17$ s showing the three-wave pattern. As expected, the Lagrangian surface contains more harmonics than the Eulerian one due to the multiple possible combinations between horizontal and vertical particles harmonics. Figure 9 shows the time evolution of the three harmonics amplitudes. Again, the Eulerian case is presented for comparison purpose showing that the BF modulation is absent.

In the presented tri-dimensional structure, we can see that sideband harmonics modulations are synchronous leading to strong opposite modulation between carrier and harmonics amplitudes. We can also see that the mean amplitude of the carrier in the Lagrangian framework is always notably smaller than the prescribed value (0.2) which is the consequence of constructive harmonics interactions. This constant decrease of the carrier amplitude is amplified by the fact that the prescribed amplitude is the orbital spectrum amplitude and not the sea surface spectrum amplitude. On the contrary, the

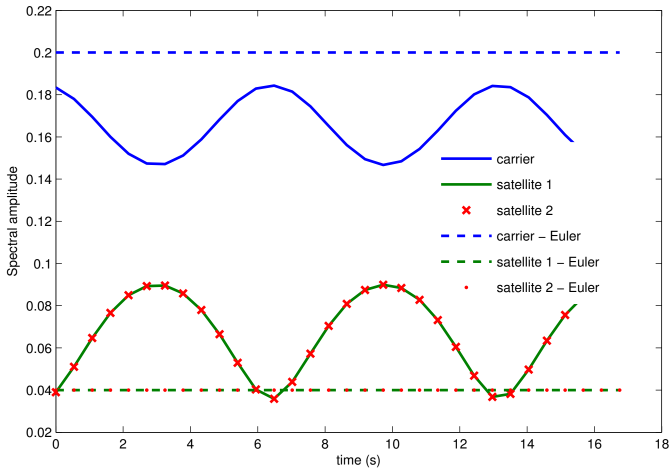

FIGURE 9. Evolution of the carrier and satellites amplitudes as a function of time.

two sideband harmonics take advantages of positive interaction permanently increasing their mean amplitudes.

Here, we have focused on the modulation-demodulation resonance that can be related to a Benjamin-Feir modulational instability. We have shown that, from a Lagrangian point of view, no energy is exchanged between the involved orbital harmonics. On the contrary, the Eulerian interpretation of this phenomenon, based on the surface spectrum analysis instead of the orbital one, is a permanent and periodical energy exchange between the carrier wave and its two sideband harmonics. This shows that the Lagrangian formulation is in a certain way a more natural and easier point of view. Moreover, in the Lagrangian framework, the time invariability of the harmonics amplitudes suggests that the side-band generation process (the instability itself) can be clearly separated from the modulational part (beating phenomena). However, it is known that asymmetric evolution of the sideband harmonics, responsible of the frequency down-shift effect, is obtained when the modulation increases and when stronger nonlinear effects or dissipation are taken into account. These phenomena are clearly absent at the Lagrangian second-order and are to be considered for future studies together with the derivation of the instability domain of an initial monochromatic Stokes wave.

7. Conclusion

In this paper, the second-order perturbation expansion in Lagrangian coordinates has been derived to study the interactions between deep-water gravity surface waves. In its compact and vector form, the proposed solution extends initial investigations (Pierson, 1961), fully recovers the classical second-order Eulerian expansion (Longuet-Higgins, 1963), and naturally includes the well-known Stokes drift velocity. As further illustrated in the case of tri-dimensional wave interactions, a residual spatial Stokes drift shall result from harmonics having the same frequency but different propagation directions. This phenomenon leads to an increase of the wave shape asymmetry along the propagation, and can be related to the development of short-crested wave patterns, as a possible first stage of formation of horse-shoe patterns. Indeed, Lagrangian second order terms shall contribute to sharpening and flattening effects, but, contrary to the first-order correction, these effects are applied in the direction perpendicular to the wave direction.

The modulation aspect of Benjamin-Feir instability is further shown to be captured as a beat effect in the Lagrangian framework. A periodic modulation emerges between the carrier and two sideband harmonics. As demonstrated, the orbital spectrum remains unchanged as the waves evolve in time, while the corresponding surface Eulerian spectrum exhibits periodical variations for the carrier and sideband harmonic amplitudes. It should be noted that the asymmetric evolution of the sideband harmonics, and the associated frequency downshift, are not recovered at this second Lagrangian order.

The extension of the proposed expansion to the case of varying depth and surface current could also follow the same formalism, and are to be considered for future investigations.

F. Nouguier would like to thank the Centre National de la Recherche Scientifique (CNRS) and Université de Toulon (chaire mixte) for their support. Part of this work was done during a long-time visit at the Laboratoire d'Oceanographie Spatiale, Ifremer Brest.

Appendix A

A.1. *Perfect differential and vorticity*

There is no vorticity if the velocity field $\boldsymbol{R}_t$ can be written in the form:

$$\boldsymbol{R}_t = \boldsymbol{\nabla} F. \tag{A 1}$$

where F is any scalar function. Noting that $dF = \boldsymbol{\nabla} F \cdot d\boldsymbol{R}$, we thus have:

$$dF = x_t\ dx + y_t\ dy + z_t\ dz. \tag{A 2}$$

Replacing terms dx, dy and dz by their respective particle label dependent expressions:

$$dx = x_\alpha d\alpha + x_\beta d\beta + x_\delta d\delta \tag{A 3}$$

$$dy = y_\alpha d\alpha + y_\beta d\beta + y_\delta d\delta \tag{A 4}$$

$$dz = z_\alpha d\alpha + z_\beta d\beta + z_\delta d\delta \tag{A 5}$$

where $d\boldsymbol{\zeta} = (d\alpha, d\beta, d\delta)$ denotes an infinitesimal label variation, we can rewrite

$$dF = (\mathbb{J}\boldsymbol{R}_t) \cdot d\boldsymbol{\zeta} \tag{A 6}$$

where $\mathbb{J}$ is defined equation (2.4). Thereby, if a function $F(\boldsymbol{\zeta},\ t)$ can be found such that dF is a perfect differential, there is no vorticity.

A.2. *Combination of first-order terms in Newton's law*

Consider the right-hand side of equation (4.1), $-\mathcal{H}(\Phi_1)\boldsymbol{\nabla}\Phi_{1tt}$, where $\mathcal{H}$ and $\boldsymbol{\nabla}$ are respectively the Hessian and the gradient operator :

$$\mathcal{H}(\Phi_1) = \begin{bmatrix} \phi_{1\alpha\alpha} & \phi_{1\alpha\beta} & \phi_{1\alpha\delta} \\ \phi_{1\alpha\beta} & \phi_{1\beta\beta} & \phi_{1\beta\delta} \\ \phi_{1\alpha\delta} & \phi_{1\beta\delta} & \phi_{1\delta\delta} \end{bmatrix} + c.c. \quad \text{and} \quad \boldsymbol{\nabla}\Phi_{1tt} = \begin{bmatrix} \phi_{1\alpha tt} \\ \phi_{1\beta tt} \\ \phi_{1\delta tt} \end{bmatrix} + c.c. \tag{A 7}$$

We can write $-\mathcal{H}(\Phi_1)\boldsymbol{\nabla}\Phi_{1tt} = \boldsymbol{S} + \boldsymbol{T}$ where $\boldsymbol{S} = (S^\alpha, S^\beta, S^\delta)$ and $\boldsymbol{T} = (T^\alpha, T^\beta, T^\delta)$ are tri-dimensional vectors :

$$\boldsymbol{S} = -\mathcal{H}(\phi_1)\boldsymbol{\nabla}\phi_{1tt} + c.c. \tag{A 8}$$

$$\boldsymbol{T} = -\mathcal{H}(\phi_1)\boldsymbol{\nabla}\phi^*_{1tt} + c.c. \tag{A 9}$$

where the star superscript '$*$' means the complex conjugate. We will investigate successively the explicit form of $\boldsymbol{S}$ and $\boldsymbol{T}$. Introducing the two kernels:

$$\mathcal{K} = \frac{1}{4}\frac{A(\boldsymbol{k})A(\boldsymbol{k'})}{kk'} e^{i(\boldsymbol{k}+\boldsymbol{k'})\cdot\boldsymbol{\xi}-i(\omega+\omega')t} e^{(k+k')\delta} \tag{A 10}$$

$$\underline{\mathcal{K}} = \frac{1}{4}\frac{A(\boldsymbol{k})A^*(\boldsymbol{k'})}{kk'} e^{i(\boldsymbol{k}-\boldsymbol{k'})\cdot\boldsymbol{\xi}-i(\omega-\omega')t} e^{(k+k')\delta} \tag{A 11}$$

and using ϕ_1 expression, the α component of $\boldsymbol{S}$ writes :

$$\begin{aligned} S^\alpha &= -\iint \left[(ik_\alpha)^2(ik'_\alpha)(-i\omega')^2 + (ik_\alpha)(ik_\beta)(ik'_\beta)(-i\omega')^2 + (ik_\alpha)kk'(-i\omega')^2\right]\mathcal{K} + c.c. \\ &= -\iint ik_\alpha gk'\left[k_\alpha k'_\alpha + k_\beta k'_\beta - kk'\right]\mathcal{K} + c.c. \\ &= \iint ik_\alpha gk'(kk' - \boldsymbol{k}\cdot\boldsymbol{k'})\mathcal{K} + c.c. \end{aligned} \tag{A 12}$$

Making use of the symmetric integration over k and k' in the second-term we can rewrite:

$$S^\alpha = \iint g\frac{ikk'}{2}\left(\frac{k_\alpha}{k} + \frac{k'_\alpha}{k'}\right)(kk' - \boldsymbol{k}\cdot\boldsymbol{k'})\mathcal{K} + c.c.. \tag{A 13}$$

The same procedure can be applied to the β component, leading to:

$$(S^\alpha, S^\beta) = \iint \ \mathcal{N}\ gkk'\frac{i(\widehat{\boldsymbol{k}} + \widehat{\boldsymbol{k'}})}{2} + c.c. \tag{A 14}$$

where $\mathcal{N}$ is defined equation (4.7). As to the δ component of $\boldsymbol{S}$, it is found to be:

$$\begin{aligned} S^\delta &= -\iint \left[(ik_\alpha)k(ik'_\alpha)(-i\omega')^2 + (ik_\beta)k(ik'_\beta)(-i\omega')^2 + k^2k'(-i\omega')^2\right]\mathcal{K} + c.c. \\ &= \iint \mathcal{N}\ gkk' + c.c. \end{aligned} \tag{A 15}$$

For the α component of $\boldsymbol{T}$,

$$T^\alpha = \iint ik_\alpha gk'(\boldsymbol{k}\cdot\boldsymbol{k'} + kk')\underline{\mathcal{K}} + c.c, \tag{A 16}$$

we invert $\boldsymbol{k}$ and $\boldsymbol{k'}$ in the *c.c.* expression to obtain:

$$T^\alpha = \iint g\frac{ikk'}{2}\left(\frac{k_\alpha}{k} - \frac{k'_\alpha}{k'}\right)(kk' + \boldsymbol{k}\cdot\boldsymbol{k'})\underline{\mathcal{K}} + c.c. \tag{A 17}$$

Applying the same technique to the β component we come up with equation (4.6) which can be written :

$$(T^\alpha, T^\beta) = \iint \frac{i(\widehat{\boldsymbol{k}} - \widehat{\boldsymbol{k'}})}{2} gkk'(\boldsymbol{k}\cdot\boldsymbol{k'} + kk')\underline{\mathcal{K}} + c.c. \tag{A 18}$$

$$= \iint \frac{i(\widehat{\boldsymbol{k}} - \widehat{\boldsymbol{k'}})}{2} gkk'\underline{\mathcal{N}} + c.c. \tag{A 19}$$

At last, the δ component of $\boldsymbol{T}$ can easily be derived as :

$$T^\delta = \iint gkk'(kk' + \boldsymbol{k}\cdot\boldsymbol{k'})\underline{\mathcal{K}} + c.c. \tag{A 20}$$

$$= \iint gkk'\underline{\mathcal{N}} + c.c. \tag{A 21}$$

A.3. *Combination of first-order terms in conservation law*

The combination of first-order terms in the conservation law (4.11) writes:

$$\Phi_{1\alpha\alpha}\Phi_{1\beta\beta}+\Phi_{1\alpha\alpha}\Phi_{1\delta\delta}+\Phi_{1\beta\beta}\Phi_{1\delta\delta}-\Phi^2_{1\alpha\beta}-\Phi^2_{1\alpha\delta}-\Phi^2_{1\beta\delta} \tag{A 22}$$

where $\Phi_1=\phi_1+\phi_1^*$. After combination of all the terms in the form $\phi_{1mn}\phi_{1pq}$ and $\phi^*_{1mn}\phi^*_{1pq}$ where m,n,p,q can be any of the variables α, β or δ we obtain:

$$\begin{aligned}
&\iint \big[(ik_\alpha)^2(ik'_\beta)^2+(ik_\alpha)^2k'^2+(ik_\beta)^2k'^2-(ik_\alpha)(ik_\beta)(ik'_\alpha)(ik'_\beta)\\
&\quad -(ik_\alpha)k(ik'_\alpha)k'-(ik_\beta)k(ik'_\beta)k'\big]\,\mathcal{K}+c.c.\\
=&\iint \left[\tfrac{1}{2}(k_\alpha k'_\beta-k_\beta k'_\alpha)^2+kk'(\boldsymbol{k}\cdot\boldsymbol{k}'-kk')\right]\mathcal{K}+c.c.\\
=&-\iint\left[kk'(1-\widehat{\boldsymbol{k}}\cdot\widehat{\boldsymbol{k}}')\frac{kk'-\boldsymbol{k}\cdot\boldsymbol{k}'}{2}\right]\mathcal{K}+c.c.\\
=&-\iint\frac{kk'-\boldsymbol{k}\cdot\boldsymbol{k}'}{2}\mathcal{N}+c.c.
\end{aligned} \tag{A 23}$$

In the same manner, the combination of the terms $\phi_{1mn}\phi^*_{1pq}$ gives:

$$-\iint\frac{kk'+\boldsymbol{k}\cdot\boldsymbol{k}'}{2}\underline{\mathcal{N}}+c.c. \tag{A 24}$$

Appendix B

In this section we prove the existence of the following integral in the sense of the Cauchy principal value:

$$\underline{\boldsymbol{r}}_2=PV\iint_{\Re^4} i\frac{\omega\boldsymbol{k}+\omega'\boldsymbol{k}'}{2(\omega-\omega')}\underline{\mathcal{B}}e^{-i(\omega-\omega')t}e^{(k+k')\delta}+c.c. \tag{B 1}$$

By definition, this can be rewritten:

$$\underline{\boldsymbol{r}}_2=\lim_{\gamma\to 0}\iint_{\Re^4-\mathcal{E}}-\frac{\mathcal{H}(\boldsymbol{k},\boldsymbol{k}')}{4(\omega-\omega')}e^{(k+k')\delta} \tag{B 2}$$

where $\mathcal{E}$ is the domain such as $|\omega-\omega'|<\gamma$ and

$$\mathcal{H}(\boldsymbol{k},\boldsymbol{k}')=(\omega\boldsymbol{k}+\omega'\boldsymbol{k}')(1+\widehat{\boldsymbol{k}}\cdot\widehat{\boldsymbol{k}}')|A(\boldsymbol{k})||A(\boldsymbol{k}')|\sin\left[(\boldsymbol{k}-\boldsymbol{k}')\cdot\boldsymbol{\xi}-(\omega-\omega')t+\varphi_{\boldsymbol{k}}-\varphi_{\boldsymbol{k}'}\right] \tag{B 3}$$

where $\varphi_{\boldsymbol{k}}$ and $\varphi_{\boldsymbol{k}'}$ are respectively the phases of $A(\boldsymbol{k})$ and $A(\boldsymbol{k}')$. We denote $\mathcal{H}^0(k,\widehat{\boldsymbol{k}},\widehat{\boldsymbol{k}}')$ the value of (B 3) when $k=k'$ $(\omega=\omega')$:

$$\mathcal{H}^0(k,\widehat{\boldsymbol{k}},\widehat{\boldsymbol{k}}')=\mathcal{H}(\boldsymbol{k},k\widehat{\boldsymbol{k}}')=\omega k(\widehat{\boldsymbol{k}}+\widehat{\boldsymbol{k}}')(1+\widehat{\boldsymbol{k}}\cdot\widehat{\boldsymbol{k}}')|A(\boldsymbol{k})||A(k\widehat{\boldsymbol{k}}')|\sin\left[k(\widehat{\boldsymbol{k}}-\widehat{\boldsymbol{k}}')\cdot\boldsymbol{\xi}+\varphi_{\boldsymbol{k}}-\varphi_{k\widehat{\boldsymbol{k}}'}\right] \tag{B 4}$$

Focusing now on the integral:

$$\underline{\boldsymbol{r}}_2^0=\lim_{\gamma\to 0}\iint_{\Re^4-\mathcal{E}}-\frac{\mathcal{H}^0(k,\widehat{\boldsymbol{k}},\widehat{\boldsymbol{k}}')}{4(\omega-\omega')}e^{(k+k')\delta} \tag{B 5}$$

and noting that $\mathcal{H}^0(k,\widehat{\boldsymbol{k}}',\widehat{\boldsymbol{k}})=-\mathcal{H}^0(k,\widehat{\boldsymbol{k}},\widehat{\boldsymbol{k}}')$ leads to a a vanishing value of $\underline{\boldsymbol{r}}_2^0$ since integration is realized over all directions of $\boldsymbol{k}$ and $\boldsymbol{k}'$. We can thus rewrite (B 2) in the form:

$$\underline{\boldsymbol{r}}_2 = \lim_{\gamma \to 0} \iint_{\Re^4 - \mathcal{E}} -\frac{\mathcal{H}(\boldsymbol{k},\boldsymbol{k}') - \mathcal{H}^0(k,\widehat{\boldsymbol{k}},\widehat{\boldsymbol{k}}')}{4(\omega-\omega')} e^{(k+k')\delta} \tag{B 6}$$

or more explicitly:

$$\underline{\boldsymbol{r}}_2 = \lim_{\gamma \to 0} \iint_{\Re^4 - \mathcal{E}} \frac{i}{4}(1+\widehat{\boldsymbol{k}}\cdot\widehat{\boldsymbol{k}}')e^{(k+k')\delta} \times \tag{B 7}$$

$$\left[\frac{(\omega\boldsymbol{k}+\omega'\boldsymbol{k}')A(\boldsymbol{k})A^*(\boldsymbol{k}')e^{i(\boldsymbol{k}-\boldsymbol{k}')\cdot\boldsymbol{\xi}-i(\omega-\omega')t} - k\omega(\widehat{\boldsymbol{k}}+\widehat{\boldsymbol{k}}')A(\boldsymbol{k})A^*(k\widehat{\boldsymbol{k}}')e^{ik(\widehat{\boldsymbol{k}}-\widehat{\boldsymbol{k}}')\cdot\boldsymbol{\xi}}}{\omega-\omega'}\right] + c.c.$$

The limit when $\omega \to \omega'$ of the term between brackets writes:

$$-ik\omega(\widehat{\boldsymbol{k}}+\widehat{\boldsymbol{k}}')A(\boldsymbol{k})A^*(k\widehat{\boldsymbol{k}}')e^{ik(\widehat{\boldsymbol{k}}-\widehat{\boldsymbol{k}}')\cdot\boldsymbol{\xi}}\ t \tag{B 8}$$

ensuring (B 2) to be a finite limit and that $\underline{\boldsymbol{r}}_2$ is integrable in the Cauchy principal value sense.

REFERENCES

Aberg, S. 2007 Wave intensities and slopes in Lagrangian seas. *Advances in Applied Probability* **39** (4), 1020–1035.

Aberg, S & Lindgren, Georg 2008 Height distribution of stochastic lagrange ocean waves. *Probabilistic Engineering Mechanics* **23** (4), 359–363.

Annenkov, S Yu & Shrira, VI 1999 Sporadic wind wave horse-shoe patterns. *Nonlinear Processes in Geophysics* **6** (1), 27–50.

Benjamin, T. Brooke & Feir, J. E. 1967 The disintegration of wave trains on deep water part 1. theory. *Journal of Fluid Mechanics* **27**, 417–430.

Buldakov, EV, Taylor, PH & Taylor, R Eatock 2006 New asymptotic description of nonlinear water waves in lagrangian coordinates. *Journal of Fluid Mechanics* **562** (1), 431–444.

Clamond, Didier 2007 On the lagrangian description of steady surface gravity waves. *Journal of Fluid Mechanics* **589**, 433–454.

Collard, F & Caulliez, G 1999 Oscillating crescent-shaped water wave patterns. *Physics of Fluids (1994-present)* **11** (11), 3195–3197.

Creamer, D.B., Henyey, F., Schult, R. & Wright, J. 1989 Improved linear representation of ocean surface waves. *Journal of Fluid Mechanics* **205**, 135–161.

Daemrich, Karl-Friedrich & Woltering, Stefan 2008 How non-linear are linear waves? In *German Joint Symposium on Hydraulic and Ocean Engineering (JOINT 2008)*.

Dias, Frédéric & Kharif, Christian 1999 Nonlinear gravity and capillary-gravity waves. *Annual review of fluid mechanics* **31** (1), 301–346.

Elfouhaily, T., Thompson, D., Vandemark, D. & Chapron, B. 1999 Weakly nonlinear theory and sea state bias estimation. *J. Geophys. Res.* **104** (C4), 7641–7647.

Fouques, Sébastien, Krogstad, Harald E & Myrhaug, Dag 2006 A second order lagrangian model for irregular ocean waves. *Journal of offshore mechanics and Arctic engineering* **128** (3), 177–183.

Fouques, Sébastien & Stansberg, Carl Trygve 2009 A modified linear lagrangian model for irregular long-crested waves. In *ASME 2009 28th International Conference on Ocean, Offshore and Arctic Engineering*, pp. 495–502. American Society of Mechanical Engineers.

Gerstner, F.J. 1809 Theorie der wellen. *Annelen der Physik* **32**.

Gjosund, S.H. 2003 A lagrangian model for irregular waves and wave kinematics. *Trans. of ASME* **125**, 94–102.

Hara, Tetsu & Mei, Chiang C. 1991 Frequency downshift in narrowbanded surface waves under the influence of wind. *Journal of Fluid Mechanics* **230**, 429–477.

Hasselmann, K. 1962 On the nonlinear energy transfer in a gravity-wave spectrum. Part 1. General theory. *J. Fluid Mech.* **12**, 481–500.

Hsu, Hung-Chu, Chen, Yang-Yih & Wang, Cyun-Fu 2010 Perturbation analysis of short-crested waves in lagrangian coordinates. *Nonlinear Analysis: Real World Applications* **11** (3), 1522–1536.

Hsu, Hung-Chu, Ng, Chiu-On & Hwung, Hwung-Hweng 2012 A new lagrangian asymptotic solution for gravity-capillary waves in water of finite depth. *Journal of Mathematical Fluid Mechanics* **14** (1), 79–94.

Kenyon, Kern E 1969 Stokes drift for random gravity waves. *Journal of Geophysical Research* **74** (28), 6991–6994.

Kinsman, B. 1965 *Wind Waves: Their Generation and Propagation on the Ocean Surface*. Prentice-Hall.

Lake, Bruce M, Yuen, Henry C, Rungaldier, Harald & Ferguson, Warren E 1977 Nonlinear deep-water waves: theory and experiment. part 2. evolution of a continuous wave train. *J. Fluid Mech* **83** (01), 49–74.

Lamb, H. 1932 *Hydrodynamics*. Cambridge University Press, London: Dover Publications.

Leblanc, S. 2004 Local stability of gerstner's waves. *Journal of Fluid Mechanics* **506**, 245–254.

Lindgren, Georg 2006 Slepian models for the stochastic shape of individual lagrange sea waves. *Advances in Applied Probability* pp. 430–450.

Lindgren, Georg & Aberg, S 2009 First order lagrange model for asymmetric ocean waves. *J. Offshore Mech. Arct* .

Lindgren, Georg & Lindgren, Finn 2011 Stochastic asymmetry properties of 3d gauss-lagrange ocean waves with directional spreading. *Stochastic Models* **27** (3), 490–520.

Longuet-Higgins, M.S. 1963 The effects of non-linearities on statistical distributions in the theory of sea waves. *Journal of Fluid Mechanics* **17**, 459–480.

Longuet-Higgins, M.S. 1987 Lagrangian moments and mass transport in stokes waves. *Journal of Fluid Mechanics* **179**, 547–55.

Longuet-Higgins, Michael S 1986 Eulerian and lagrangian aspects of surface waves. *Journal of Fluid Mechanics* **173**, 683–707.

Naciri, M. & Mei, C.C. 1992 Evolution of a short surface wave on a very long surface wave of finite amplitude. *Journal of Fluid Mechanics* **235**, 415–452.

Nouguier, F., Guérin, C.A. & Chapron, B. 2009 'Choppy wave' model for nonlinear gravity waves. *Journal of Geophysical Research (Oceans)* **114** (C13), 09012.

Phillips, Owen M 1977 *The dynamics of the upper ocean*. Cambridge university press.

Pierson, WJ 1961 Models of random seas based on the lagrangian equations of motion. *Tech. Rep.*. New York Univ., Coll. of Eng. Res. Div., Dept. of Meteorology and Oceanography, tech. Rep. prepared for the Office of Naval Research under contract Nonr-285(03).

Segur, Harvey, Henderson, Diane, Carter, John, Hammack, Joe, Li, Cong-Ming, Pheiff, Dana & Socha, Katherine 2005 Stabilizing the benjamin-feir instability. *Journal of Fluid Mechanics* **539**, 229–272.

Shemer, L 2010 On benjamin-feir instability and evolution of a nonlinear wave with finite-amplitude sidebands. *Natural Hazards and Earth System Science* **10** (11), 2421–2427.

Shrira, Victor I, Badulin, Sergei I & Kharif, Christian 1996 A model of water wave 'horse-shoe'patterns. *Journal of Fluid Mechanics* **318**, 375–405.

Socquet-Juglard, Hervé, Dysthe, Kristian, Trulsen, Karsten, Krogstad, Harald E & Liu, Jingdong 2005 Probability distributions of surface gravity waves during spectral changes. *Journal of Fluid Mechanics* **542**, 195–216.

Stoker, J.J. 1957 Water waves. *New York* .

Stokes, G.G. 1847 On the theory of oscillatory waves. *Trans. Camb. Phil. Soc* **8** (441), 197–229.

Su, Ming-Yang, Bergin, Mark, Marler, Paul & Myrick, Richard 1982 Experiments on nonlinear instabilities and evolution of steep gravity-wave trains. *Journal of Fluid Mechanics* **124**, 45–72.

Weber, B.L. & Barrick, D.E. 1977 On the nonlinear theory for gravity waves on the ocean's surface. *J. Phys. Oceanogr.* **7** (1).

Yakubovich, E. I. & Zenkovich, D. A. 2004 Matrix approach to lagrangian fluid dynamics. *Journal of Fluid Mechanics* **443**, 167–196.

Zakharov, Vladimir E 1968 Stability of periodic waves of finite amplitude on the surface of a deep fluid. *Journal of Applied Mechanics and Technical Physics* **9** (2), 190–194.